Cell Stem Cell
Short Article

Generation of Rejuvenated Antigen-Specific T Cells by Reprogramming to Pluripotency and Redifferentiation

Toshinobu Nishimura,[1] Shin Kaneko,[1,9,*] Ai Kawana-Tachikawa,[2] Yoko Tajima,[1] Haruo Goto,[1] Dayong Zhu,[2] Kaori Nakayama-Hosoya,[2] Shoichi Iriguchi,[1] Yasushi Uemura,[6] Takafumi Shimizu,[1] Naoya Takayama,[3,10] Daisuke Yamada,[7] Ken Nishimura,[8] Manami Ohtaka,[8] Nobukazu Watanabe,[4] Satoshi Takahashi,[5] Aikichi Iwamoto,[2] Haruhiko Koseki,[7] Mahito Nakanishi,[8] Koji Eto,[3,10] and Hiromitsu Nakauchi[1,*]

[1]Division of Stem Cell Therapy, Center for Stem Cell Biology and Regenerative Medicine
[2]Division of Infectious Diseases, Advanced Clinical Research Center
[3]Stem Cell Bank, Center for Stem Cell Biology and Regenerative Medicine
[4]Laboratory of Diagnostic Medicine, Center for Stem Cell Biology and Regenerative Medicine
[5]Division of Molecular Therapy, Advanced Clinical Research Center
The Institute of Medical Science, The University of Tokyo, 4-6-1 Shirokanedai, Minato-ku, Tokyo 108-8639, Japan
[6]Division of Immunology, Aichi Cancer Center Research Institute, 1-1 Kanakoden, Chikusa-ku Nagoya, Aichi 464-8681, Japan
[7]Laboratory for Lymphocyte Development, RIKEN Center for Allergy and Immunology, 1-7-22 Suehiro-cho, Tsurumi-ku, Yokohama, Kanagawa 230-0045, Japan
[8]Research Center for Stem Cell Engineering, National Institute of Advanced Industrial Science and Technology, 1-1-1 Higashi, Central 4, Tsukuba, Ibaraki 305-8562, Japan
[9]Present address: Department of Fundamental Cell Technology, Center for iPS Cell Research and Application (CiRA), Kyoto University, 53 Kawahara-cho, Shogoin, Sakyo-ku, Kyoto 606-8507, Japan
[10]Present address: Department of Clinical Application, CiRA, Kyoto University, 53 Kawahara-cho, Shogoin, Sakyo-ku, Kyoto 606-8507, Japan
*Correspondence: kaneko.shin@cira.kyoto-u.ac.jp (S.K.), nakauchi@ims.u-tokyo.ac.jp (H.N.)
http://dx.doi.org/10.1016/j.stem.2012.11.002

SUMMARY

Adoptive immunotherapy with functional T cells is potentially an effective therapeutic strategy for combating many types of cancer and viral infection. However, exhaustion of antigen-specific T cells represents a major challenge to this type of approach. In an effort to overcome this problem, we reprogrammed clonally expanded antigen-specific $CD8^+$ T cells from an HIV-1-infected patient to pluripotency. The T cell-derived induced pluripotent stem cells were then redifferentiated into $CD8^+$ T cells that had a high proliferative capacity and elongated telomeres. These "rejuvenated" cells possessed antigen-specific killing activity and exhibited T cell receptor gene-rearrangement patterns identical to those of the original T cell clone from the patient. We also found that this method can be effective for generating specific T cells for other pathology-associated antigens. Thus, this type of approach may have broad applications in the field of adoptive immunotherapy.

INTRODUCTION

T cells play a central role in acquired immunity and the configuration of systemic immunity against pathogens. In particular, cytotoxic T lymphocytes (CTLs) are major components of this systemic response to microorganisms, viral infections, and neoplasms (Greenberg, 1991; Zhang and Bevan, 2011). T cells initiate their proliferative and effector functions upon human leukocyte antigen (HLA)-restricted recognition of specific antigen peptides via T cell receptors (TCRs). This is greatly beneficial in enabling the selective recognition and eradication of target cells, and also in long-term immunological surveillance by long-lived memory T cells (Butler et al., 2011; Jameson and Masopust, 2009; MacLeod et al., 2010). However, viruses in chronic infection or cancers often hamper or escape the T cell immunity by decreasing the expression of molecules required for T cell recognition or by inhibiting antigen presentation (Virgin et al., 2009). In addition, continuous exposure to chronically expressed viral antigens or cancer/self-antigens can drive T cells into an "exhausted" state. This is characterized by loss of effector functions and the potential for long-term survival and proliferation, ultimately leading to the depletion of antigen-responding T cell pools (Klebanoff et al., 2006; Wherry, 2011).

The infusion of ex vivo-expanded autologous antigen-specific T cells is being developed clinically for T cell immunotherapy. However, up to now, highly expanded T cells have not proven to be particularly effective (June, 2007). This is in part explained by losses of function that occur during the ex vivo manipulation of patient autologous T cells. In another instance, genetic modification of antigen receptors is an ambitious but only partially successful way to add desired antigen specificity to nonspecific T cells (Morgan et al., 2006; Porter et al., 2011). The therapeutic effect also strongly depends on the extent of functional loss that occurs during the ex vivo manipulation of T cells and on the stability of exogenous antigen receptor expression specific to target molecules in the presence of the endogenous TCR genes (Bendle et al., 2010; Brenner and Okur, 2009).

For the purpose of overcoming these obstacles, the therapeutic potential of induced pluripotent stem cells (iPSCs) is being

explored. Embryonic stem cells (ESCs) or iPSCs have the capacity for self-renewal while maintaining pluripotency (Takahashi et al., 2007) and could potentially form the basis for the unlimited induction of antigen-specific juvenile T cells. However, there are challenges to this approach as well, given that methods for the differentiation and immunological education of ESCs and iPSCs, or indeed that of intermediate hematopoietic stem and/or progenitor cells, into fully matured functional human T cells are not well established (Timmermans et al., 2009). Reprogramming the nuclei of lymphocytes was historically performed for studying whether terminally differentiated or fully matured somatic cells could revert to a pluripotent state. The first demonstration of lymphocyte reprogramming employed somatic cell nuclear transfer in murine B and T cells, proving that terminally differentiated somatic cells were reprogrammable (Hochedlinger and Jaenisch, 2002). Reprogramming murine B cells into pluripotent stem cells by iPSC technology also provided definite proof for fate reversibility in fully matured somatic cells (Hanna et al., 2008). From another point of view, nuclear reprogramming of lymphocytes is seen as having applications for regenerative medicine different than those for scientific research. The irreversible rearrangement of genes encoding immunoglobulins and TCRs was recognized solely as a genetic marker in somatic cell nuclear transfer and iPSC research. However, the preserved rearrangements in genomic DNA can also provide a blueprint of "educated" weapons for attacking cancers and pathogens in adoptive immunotherapy. Although several groups have reported the generation of T cell-derived iPSCs (T-iPSCs), their clinical applications have yet to be thoroughly explored (Brown et al., 2010; Loh et al., 2010; Seki et al., 2010; Staerk et al., 2010).

In the present study, we chose a T cell clone specific to an HIV type 1 (HIV-1) epitope of known structure to act as a generic representation of iPSC-mediated T cell regeneration. We successfully induced iPSCs from antigen-specific T cells and redifferentiated them into functional T cells. This may act as proof of concept for the application of "rejuvenated" T cells in treating various diseases. Crucial to this concept was that T-iPSCs retained the assembled "endogenous" TCR genes even after being subjected to nuclear reprogramming. Furthermore, redifferentiated T cells showed the same pattern of TCR gene arrangement as that in the original T cells. These features may therefore serve as the foundation for the reproduction of unlimited numbers of T cells that express desired TCRs conferring to antigen specificity.

RESULTS

Reprogramming an Antigen-Specific Cytotoxic T Cell Clone into Pluripotency

To establish T cell-derived iPSCs, we magnetically separated the $CD3^+$ T cell population from peripheral blood mononuclear cells (PBMCs) of healthy volunteers. The isolated $CD3^+$ T cells were stimulated with human CD3 and CD28 antibody-coated microbeads (α-CD3/28 beads) in the presence of interleukin-2 (IL-2). We then transduced the activated $CD3^+$ T cells with separate retroviral vectors that individually code for *OCT3/4*, *SOX2*, *KLF4*, and c-*MYC*. Human ESC-like colonies were obtained within 25 days of culture (Figure S1A available online).

We also isolated PBMCs from an HLA-A24-positive patient with a chronic HIV-1 infection. $CD8^+$ CTL clones specific for an antigenic peptide (amino acids [aa] 138–145) from the HIV-1 Nef protein (Nef-138-8(WT); RYPLTFGW) (Altfeld et al., 2006) were established. One of the clones, H25-#4, was stimulated using α-CD3/28 beads in the presence of IL-2 and then transduced simultaneously with six retroviral vectors encoding *OCT3/4*, *SOX2*, *KLF4*, c-*MYC*, *NANOG*, and *LIN28A*. However, we could not reprogram H25-#4 into pluripotency, possibly due to the cells being in a low infectious and exhausted state, or due to insufficient expression of the reprogramming factors. In response, we attempted to increase transduction efficiency and transgene expression by using two Sendai virus (SeV) vectors. One of them encodes tetracistronic factors (*OCT3/4*, *SOX2*, *KLF4*, and c-*MYC*) (Nishimura et al., 2011) with the miR-302 target sequence (SeVp[KOSM302L]; K.N., M.O., and M.N., data not shown), and another encodes SV40 large T antigen (SeV18[T]) (Fusaki et al., 2009). After transduction of phytohemagglutinin (PHA)-activated H25-#4 cells with the SeV vectors in the presence of IL-7 and IL-15, sufficient numbers of human ESC-like colonies appeared within 40 days of culture (Figure 1A). Use of this SeV system and optimization of transduction conditions greatly improved the reprogramming efficiency. It enabled us to reprogram several $CD8^+$ or $CD4^+$ T cell clones specific to pp65 antigen in cytomegalovirus (CMV), glutamic acid decarboxylase (GAD) antigen in type 1 diabetes, and α-GalCer (Table 1).

The resultant $CD3^+$ T cell- and H25-#4-derived ESC-like colonies (TkT3V1-7 and H254SeVT-3, respectively) exhibited alkaline phosphatase (AP) activity and expressed the pluripotent cell markers SSEA-4, Tra-1-60, and Tra-1-81 (Figures S1B–S1E and 1B–1E). H254SeVT-3 expressed HLA-A24 (Figure 1F). Both TkT3V1-7 and H254SeVT-3 also expressed human ESC-related genes (Figures S1F and 1G). The expression of exogenous reprogramming factors from the integrated provirus (TkT3V1-7) was halted (Figure S1F), and nonintegrated SeV genomic RNA was successfully removed from the cytosol by RNAi or by self-degradation caused by temperature-sensitive mutations (H254SeVT-3) (Figure 1H). Comparison of gene-expression profiles revealed that the gene-expression patterns in the ESC-like cells were similar to those in human ESCs, but differed significantly from those in peripheral blood (PB) T cells (Figure S1G). Scant methylation of the *OCT3/4* and *NANOG* promoter regions was confirmed using bisulfite PCR, thus indicating successful reprogramming (Freberg et al., 2007) (Figures S1H and 1I). In addition, when injected into nonobese diabetic severe combined immunodeficient (NOD-Scid) mice, those cells formed teratomas containing characteristic tissues derived from all three germ layers, which is indicative of pluripotency (Brivanlou et al., 2003) (Figures S3 and 2A). Therefore, those colonies were confirmed as typical human iPSCs.

T-iPSCs Carry Preassembled TCR Genes from the Original T Cell

Almost all TCRs are composed of heterodimerically associated α and β chains. *TCRA* or *TCRB* gene (encoding α chain or β chain, respectively) rearrangements are involved in normal αβ T cell development in the thymus. These rearrangements enabled us to determine retrospectively whether the iPSCs were derived from an αβ T cell. The BIOMED-2 consortium designed multiplex-PCR primers for analyzing *TCRB* gene assemblies (van Dongen et al., 2003), and we designed the primers for detecting *TCRA*

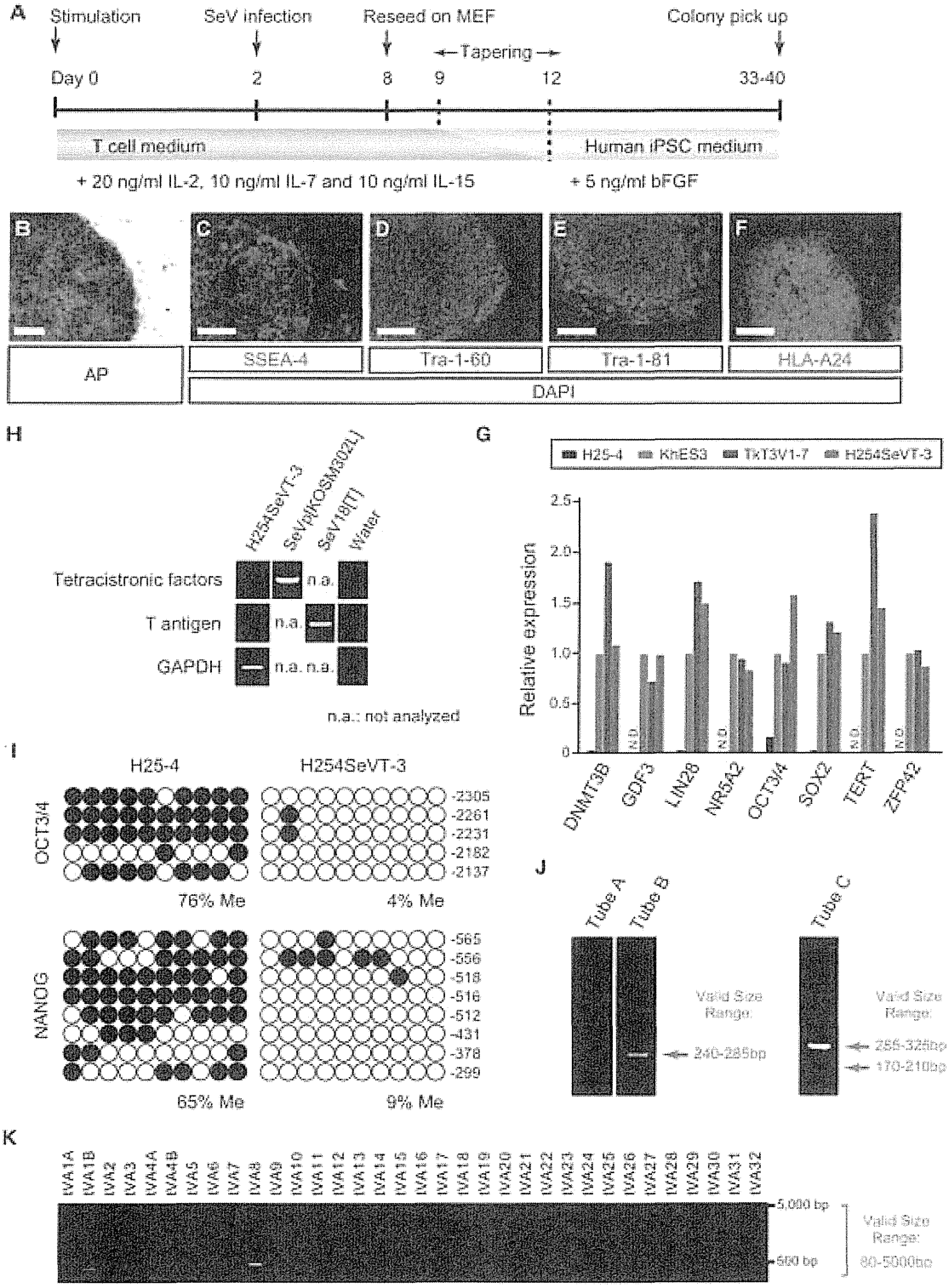

Figure 1. Generation of Human iPSCs from a CTL Clone

(A) Schematic illustration showing the generation of T-iPSCs from H25-#4 T cells using SeV vectors encoding polycistronic *OCT3/4*, *SOX2*, *KLF4*, and c-*MYC*, or SV40 large T antigen. The "tapering" indicates the gradual replacement of culture medium with human iPSC medium.

(B–F) AP activity (B) and expression of pluripotency markers (SSEA-4, C; Tra-1-60, D; and Tra-1-81, E) and HLA-A24 (F) in H254SeVT-3 cells. Nuclei were counterstained with DAPI. The scale bar represents 200 μm.

(G) Quantitative PCR for pluripotency genes in H25-#4, KhES3, TkT3V1-7, and H254SeVT-3 cells. Individual PCR reactions were normalized against 18S ribosomal RNA (rRNA).

(legend continued on next page)

Table 1. Generation of Human T-iPSCs from Various Patient-Derived T Cell Specimens

Antigen	T Cell Source	Initial Cell Number	No. of ESC-like Colonies	No. of Colonies Picked up for Establishing T-iPSC Clones	Date (MM/YYYY)
HIV-1 Nef	monoclonal T cell clone	4×10^5	7	7	05/2011
CMV pp65	polyclonal tetramer-sorted cells	~5,000	15	15	07/2011
GAD	monoclonal T cell clone	1×10^6	>100	not picked up	08/2012
		5×10^5	>100	19	08/2012
α-GalCer	FACS-sorted Vα24$^+$ cells	1×10^6	>100	not picked up	08/2012
		5×10^5	>100	7	08/2012

Sample cells were transduced with *OCT3/4*, *SOX2*, *KLF4*, *c-MYC*, and *SV40* large T-antigen by using two Sendai virus (SeV) vectors (SeVp [KOSM302L] and SeV18[T]). After around 40 days, the number of embryonic stem cell (ESC)-like colonies were counted on the basis of morphology and alkaline phosphatase (AP) activity. All established T cell-derived induced pluripotent stem cell (T-iPSC) lines were free from residual SeV vectors (one example in the case of the HIV-1 Nef-specific T-iPSC clone is shown in Figure 1H). CMV, cytomegalovirus; GAD, glutamic acid decarboxylase; FACS, fluorescence-activated cell sorting.

gene assemblies (Figure S2). *TCRB* and *TCRA* gene assemblies were identified as single bands representing each allele in TkT3V1-7 and H254SeVT-3 (Figures S1H, S1I, 1J, and 1K).

We next confirmed the presence of an antigen-recognition site on the TCR that consisted of three complementarity-determining regions (CDR1, CDR2, and CDR3). CDR3 is the most diversifiable among the three because it spans the V(D)J-junction region, where several random nucleotides (N or P nucleotides) are inserted (Alt and Baltimore, 1982; Lafaille et al., 1989). We determined the CDR3 sequences of the assembled *TCRA* and *TCRB* genes in TkT3V1-7 and H254SeVT-3 and identified a set of productive *TCRA* and *TCRB* gene rearrangements (i.e., in-frame junction with no stop codon) (Table S1 and Table 2). Furthermore, the sequences of CDR3 from H254SeVT-3 and H25-#4 were completely identical at both *TCRA* and *TCRB* gene loci. These results indicated that the iPSCs established were derived from a single T cell and that the antigen specificity encoded in the genomic DNA of the T cell was conserved during reprogramming.

Redifferentiation of T-iPSCs into CD8 Single-Positive T Cells Expressing the Desired TCR

Following the application of specific in vitro differentiation protocols, iPSCs can give rise to mesoderm-derived cell types, especially hematopoietic stem and/or progenitor cells (Takayama et al., 2008; Vodyanik et al., 2005) (Figure 2B). This was applied to assess the capacity of T-iPSCs for hematopoietic differentiation by coculturing on C3H10T1/2 feeder cells in the presence of VEGF, SCF, and FLT-3L for the generation of CD34$^+$ hematopoietic stem and/or progenitor cells. On day 14 of culture, the cells were transferred onto Delta-like 1-expressing OP9 (OP9-DL1) feeder cells (Timmermans et al., 2009) and were cocultured in the presence of FLT-3L and IL-7 (Ikawa et al., 2010) (Figure 2B). After 21–28 days of culture, the hematopoietic cells differentiated into CD45$^+$, CD38$^+$, CD7$^+$, CD45RA$^+$, CD3$^+$, and TCRαβ$^+$ T lineage cells (Figure S4). As was the case with TCRαβ transgenic mice (Borgulya et al., 1992) and chimeric mice derived from ESCs produced through nuclear transplantation of T cells (Serwold et al., 2007), aberrant expression of TCRαβ was observed at the CD4/CD8 double-negative (DN) stage. Although some of these T lineage cells differentiated into the CD4/CD8 double-positive (DP) stage and the more mature CD4 or CD8 single-positive (SP) stages (Figure 2C), we could not characterize the small number of SP cells in more detail.

During thymocyte development, the CD4/CD8 DN and DP stages correspond respectively to the *TCRB*-encoded β chain and *TCRA*-encoded α chain assembly stages (von Boehmer, 2004). In the *TCRB* locus, the negative-feedback regulation of gene assembly and the capacity to deter further rearrangement are very strict (Khor and Sleckman, 2002). In the *TCRA* locus, by contrast, negative-feedback regulation is relatively loose, and further gene assembly of the preassembled gene, a phenomenon known as "receptor revision," tends to occur (Huang and Kanagawa, 2001; Krangel, 2009). In experiments using TCRα transgenic mice, the reactivation of *Rag1* and *Rag2*, genes related to recombination machinery, occurred in CD4/CD8 DP-stage thymocytes, and gene assembly of endogenous *Tcra* was observed (Padovan et al., 1993; Petrie et al., 1993). Such further gene assembly would be exceedingly undesirable for our purposes, because it would probably convert the tropism of the TCR and render the redifferentiated T cells incapable of attacking the previously targeted antigen. To determine whether such receptor revision could occur in redifferentiating T lineage cells, we collected CD1a$^-$ DN- and CD1a$^+$ DP-stage cells from among the CD45$^+$, CD3$^+$, TCRαβ$^+$, and CD5$^+$ T lineage cells and then analyzed the gene rearrangement of TCR messenger RNAs (mRNAs) (Figures S5A–S5C). Nucleotide sequences of *TCRB* mRNAs in the T lineage cells were identical to those in

(H) Detection of the remnants of SeV genomic RNAs by RT-PCR. Each column represents the template cDNA synthesized from H254SeVT-3 cells, SeVp [KOSM302L] virus solution, and SeV18[T] virus solution. cDNAs from virus solution were the positive controls.

(I) Bisulfite sequencing analyses of the *OCT3/4* and *NANOG* promoter regions in H25-#4 and H254SeVT-3 cells. White and black circles represent unmethylated and methylated (Me) CpG dinucleotides, respectively.

(J) Multiplex PCR analysis to detect *TCRB* gene rearrangements in the H254SeVT-3 genome. Tubes A and B contain Vβ-(D)Jβ assemblies; Tube C contains D-Jβ assemblies.

(K) Multiplex PCR analysis for detection of *TCRA* gene rearrangements (V-Jα assemblies).

See Figures S1, S2, and S3 for additional data.

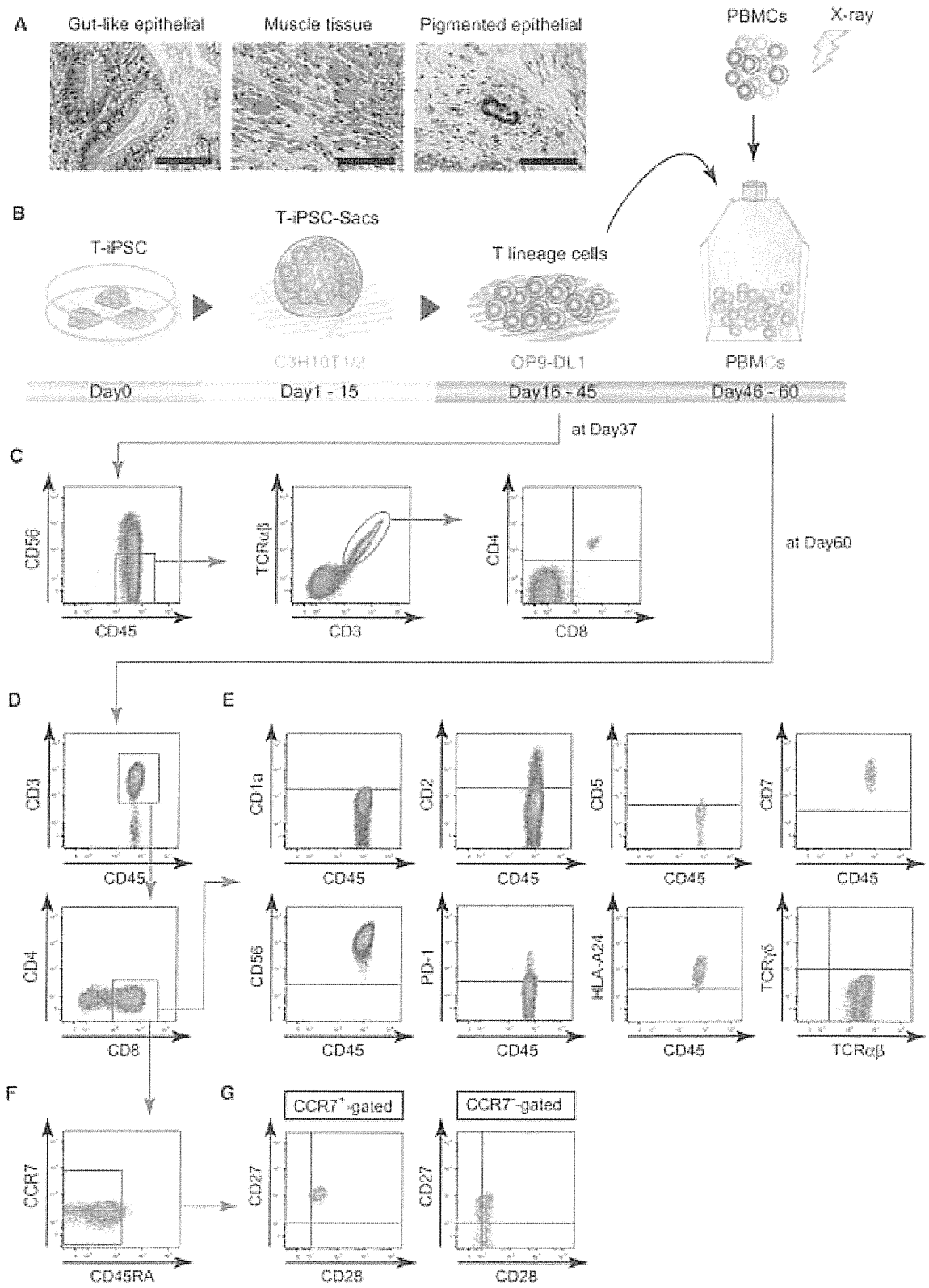

Figure 2. Redifferentiation of T-iPSCs into T Cells

(A) Representative hematoxylin- and eosin-stained sections of a teratoma formed in a NOD/ShiJic-*scid* mouse testis. H254SeVT-3 differentiated into cell lineages derived from endoderm (goblet cells in gut-like epithelial), mesoderm (smooth myocytes in muscle tissue), and ectoderm (retina cells in pigmented epithelial). The scale bar represents 100 μm.

(legend continued on next page)

the T-iPSCs at both the DN and DP stages. By contrast, some *TCRA* mRNAs at the DN and DP stages were identical to those in the T lineage cells, but others differed, and differing sequences were observed more frequently at the DP stage than the DN stage (Table S2). *RAG1* and *RAG2* expression were observed at both the DN and the DP stages, though stronger expression was observed at the DP stage (Figure S5D).

To create mature CD8 SP cells from T-iPSC-derived T lineage cells without receptor revision, we focused on TCR signaling. Turka et al. (1991) reported that TCR signaling via peptide-major histocompatibility complex (MHC) complexes during positive selection ends expression of *RAG* genes and prevents further assembly of TCR genes. They also showed that mimicking TCR signaling using CD3 antibodies had the same effect. Therefore, we tried to stimulate the TCRs of redifferentiating T lineage cells before the completion of the DN-to-DP transition (Figure 2B). For this experiment, we cultured T lineage-committed cells on OP9-DL1, stimulated them with α-CD3/28 beads or PHA (we defined this as the first stimulation) and then cocultured them with irradiated HLA-A24$^-$ PMBCs in the presence of IL-7 and IL-15, which are required for the generation of memory phenotype CD8$^+$ T cells (Kaneko et al., 2009; Prlic et al., 2002; Tan et al., 2002). After 14 days, CD8 SP cells appeared (Figure 2D). These were deemed to be derivatives of H254SeV-3 based on their expression of HLA-A24 (Figure 2E). These CD8 SP cells did not express the immature thymocyte marker CD1a, but they were positive for CD56, which is expressed on CD8$^+$ T cells cultured in vitro (Lu and Negrin, 1994). In addition, these cells expressed CD7 and some CD2, but not CD5. On the one hand, they did not express PD-1, a marker of exhausted T cells (Figure 2E). On the other hand, some of them expressed the memory T cell markers CCR7, CD27, and CD28 simultaneously, thus representing a central memory T cell phenotype (Figures 2F and 2G) (Romero et al., 2007).

To test whether the redifferentiated CD8 SP cells would recognize the same epitope on the same HLA, the entire population of redifferentiated T cells was mixed with the A24/Nef-138-8(WT) tetramer and subjected to flow-cytometric analysis (Kawana-Tachikawa et al., 2002). Most of the CD8 SP cells were stained positively by the A24/Nef-138-8(WT) tetramer, but not by the control tetramer, which represents HIV-1 envelope-derived peptides (RYLRDQQLL; Figure 3A and data not shown). We then collected the A24/Nef-138-8(WT) tetramer-reactive CD8$^+$ cells and expanded them once again using α-CD3/28 beads or PHA stimulation (defined as the second stimulation; Figure 3A). Finally, after several independent redifferentiation experiments, we obtained A24/Nef-138-8(WT) tetramer-reactive CD8 SP cells (reT-1, reT-2.1, reT-2.2, and reT-3). As expected, sequence analysis of *TCRA* and *TCRB* mRNAs in the redifferentiated CD8 SP cells revealed that the TCR gene rearrangement pattern was identical to that in the H25-#4 original T cell clone (Figure 3B and Table 1).

To determine whether the redifferentiated CD8 SP cells were of the T cell lineage, we used quantitative PCR to compare gene-expression profiles among redifferentiated CD8 SP cells, PB CD4$^+$ and CD8$^+$ T cells, and the H25-#4 original T cell clone. As shown in Figure 3C, the expression patterns of CD3, CD4, and CD8 were similar among PB CD8$^+$ T cells, redifferentiated CD8 SP cells, and the H25-#4 original T cell clone. However, the pattern differed from those in PB CD4$^+$ T cells (Figure 3C). Cytotoxic "signature" genes such as granzyme B (*GZMB*), perforin (*PRF1*), interferon-γ (IFN-γ; *IFNG*), and FAS ligand (*FASLG*) were expressed in PB CD8$^+$ T cells. These genes were also expressed relatively strongly in redifferentiated CD8 SP cells and in the H25-#4 original T cell clone; that is, in already-primed T cells (Figure 3D). The expression patterns of several factors involved in transcription or signal transduction and of cell-surface molecules were similar among PB CD8$^+$ T cells, redifferentiated CD8 SP cells, and the H25-#4 original T cell clone (Figure 3E). To exclude the possibility that the redifferentiated CD8 SP cells had acquired natural killer (NK)-like properties during their coculture with OP9-DL1 or PBMCs, we used a complementary DNA (cDNA) microarray to analyze global gene-expression profiles in redifferentiated CD8 cells, the H25-#4 original T cell clone, and PB NK cells. Correlation and cluster analyses of the gene-expression profile of the redifferentiated CD8 SP cells showed it to be similar to that of the H25-#4 original T cell clone but different from that of NK cells (Figures 3F and 3G). These data strongly suggest that T-iPSCs are able to redifferentiate into CD8$^+$ T cells that exhibit the same antigen specificity as that of the original T cell.

Generation of Highly Proliferative T Cells through T-iPSCs

Fewer than 10^5 T lineage cells were obtained from ~3 × 10^5 T-iPSCs after coculture with C3H10T1/2 and OP9-DL1 cells. However, they could be expanded to >10^8 cells with the first stimulation (data not shown). After separating A24/Nef-138-8(WT) tetramer-reactive CD8$^+$ cells, we assessed the expansion rate induced by the second stimulation and also assessed the establishment of reT-1, reT-2.2, and reT-3. We found that these cells expanded from 100-fold to 1,000-fold within 2 weeks in the presence of IL-7 and IL-15, whereas the H25-#4 original T cell clone expanded only about 20-fold (Figure 4A). Even after 100-to-1,000-fold expansions, some cells still expressed central memory T cell markers such as CCR7, CD27, and CD28 (Figure S6). Perhaps with passage through the iPSC state, wherein telomerase activity is quite high (Marion et al., 2009; Takahashi et al., 2007), re-elongation of shortened telomeres in the H25-#4 original T cell clone gives the redifferentiated T cells high replicative potential (Monteiro et al., 1996; Weng et al., 1998). In fact, the redifferentiated T cells carried longer telomeres than the original T cell clone (Figure 4B), an overall process that we call

(B) Schematic illustration of redifferentiation from T-iPSCs into T cells.
(C) Flow-cytometric analysis of the phenotypes of differentiating T lineage cells at 37 days after starting redifferentiation.
(D and E) Flow-cytometric analysis of the phenotypes of T cells at 60 days after starting redifferentiation. Fluorescence-activated cell sorting (FACS) analyses revealed CD8 single-positive maturation (D) and expression of several T cell markers (E).
(F and G) Memory phenotypes of redifferentiated CD8$^+$ T cells. There existed memory-phenotyped cells such as all positive for CCR7 (F), CD27, and CD28 (G). Data are representative of at least three independent experiments. See Figures S3, S4, and S5 and Table S2 for additional data.

Table 2. TCR Gene Rearrangements in H25-4, H254SeVT-3, or Redifferentiated CD8$^+$ T Cells

Cell	Genome or mRNA	Productivity	Rearrangement			Sequence of Junctional Region		
			Vα		Jα	3′Vα	P(N)	5′Jα
TCRA								
H25-4	genome	productive	TRAV8-3*01		TRAJ10*01	TGTGCTGTGGGT	T	TCACGGGAGGAGGAAACAAACTC ACCTTTT
		unproductive[a]	TRAV13-1*01		TRAJ29*01	TGTGCAGCAA	TCC	TCAGGAAACACACCTCTTGTCTTT
H254SeVT-3	genome	productive	TRAV8-3*01		TRAJ10*01	TGTGCTGTGGGT	T	TCACGGGAGGAGGAAACAAACTC ACCTTTT
		unproductive[a]	TRAV13-1*01		TRAJ29*01	TGTGCAGCAA	TCC	TCAGGAAACACACCTCTTGTCTTT
reT-1	mRNA	productive	TRAV8-3*01		TRAJ10*01	TGTGCTGTGGGT	T	TCACGGGAGGAGGAAACAAACTC ACCTTTT
		unproductive[a]	TRAV13-1*01		TRAJ29*01	TGTGCAGCAA	TCC	TCAGGAAACACACCTCTTGTCTTT
reT-2.1	mRNA	productive	TRAV8-3*01		TRAJ10*01	TGTGCTGTGGGT	T	TCACGGGAGGAGGAAACAAACTC ACCTTTT
		unproductive[a]	TRAV13-1*01		TRAJ29*01	TGTGCAGCAA	TCC	TCAGGAAACACACCTCTTGTCTTT
reT-3	mRNA	productive	TRAV8-3*01		TRAJ10*01	TGTGCTGTGGGT	T	TCACGGGAGGAGGAAACAAACTC ACCTTTT
		unproductive[a]	TRAV13-1*01		TRAJ29*01	TGTGCAGCAA	TCC	TCAGGAAACACACCTCTTGTCTTT
			Vβ	Dβ	Jβ	3′Vβ	N1-Dβ-N2	5′Jβ
TCRB								
H25-4	genome	productive	TRBV7-9*01	TRBD1*01	TRBJ2-5*01	TGTGCCAGCAGCTTA	CGGGACAGGGTGCCG	GAGACCCAGTACTTC
		unproductive	germline	TRBD1*01	TRBJ2-7*01	TACAAAGCTGTAACATTGTG	GGGACAACT	CTACGAGCAGTACTTCGGGCCG
H254SeVT-3	genome	productive	TRBV7-9*01	TRBD1*01	TRBJ2-5*01	TGTGCCAGCAGCTTA	CGGGACAGGGTGCCG	GAGACCCAGTACTTC
		unproductive	germline	TRBD1*01	TRBJ2-7*01	TACAAAGCTGTAACATTGTG	GGGACAACT	CTACGAGCAGTACTTCGGGCCG
reT-1	mRNA	productive	TRBV7-9*01	TRBD1*01	TRBJ2-5*01	TGTGCCAGCAGCTTA	CGGGACAGGGTGCCG	GAGACCCAGTACTTC
reT-2.1	mRNA	productive	TRBV7-9*01	TRBD1*01	TRBJ2-5*01	TGTGCCAGCAGCTTA	CGGGACAGGGTGCCG	GAGACCCAGTACTTC
reT-3	mRNA	productive	TRBV7-9*01	TRBD1*01	TRBJ2-5*01	TGTGCCAGCAGCTTA	CGGGACAGGGTGCCG	GAGACCCAGTACTTC

PCR-amplified samples (H25-4: not shown; H254SeVT-3: shown in Figures 1J and 1K; reT-1, reT-2.1, and reT-3: shown in Figure 3B) were sequenced, then V, D, and J segment usages and junctional sequences in CDR3 were identified. Following reprogramming and redifferentiation, there were no alterations in gene rearrangement in either allele at the *TCRA* and *TCRB* gene loci. See Table S1 for additional data on another T-iPSC clone (TkT3V1-7).

[a]Out-of-frame junction (at CDR3).

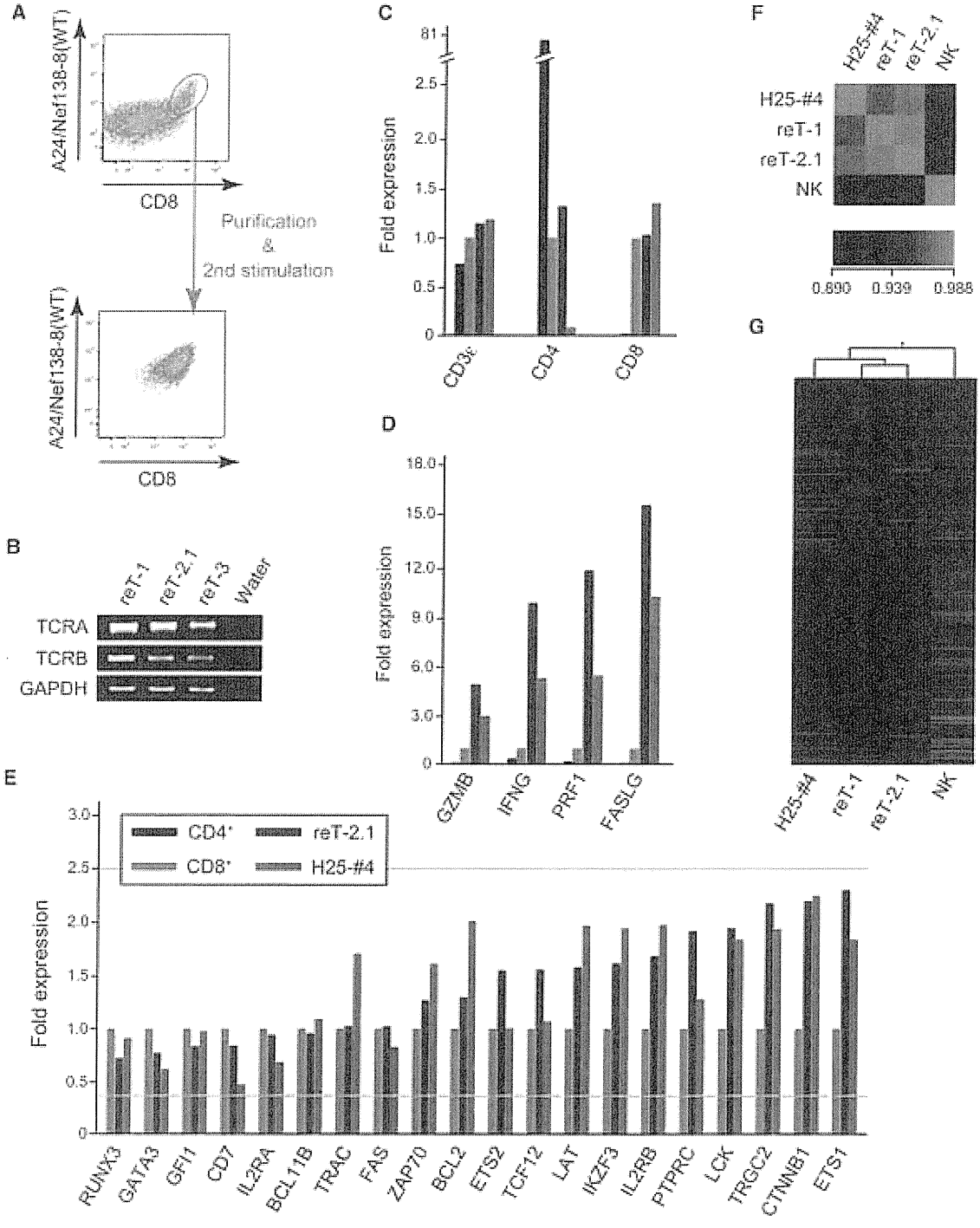

Figure 3. Characterizations of Redifferentiated T Cells as T Cells

(A) Recognition of A24/Nef-138-8(WT) tetramer at 50–60 days after starting redifferentiation, analyzed by flow cytometry (upper panel). Tetramer-positive cells were sorted by FACS or magnetically selected, then cultured for an additional 14 days, after which the expanded T cells were reanalyzed for tetramer (lower panel).

(B) TCR mRNAs were identified in a SMART-mediated cDNA library for reT-1, reT-2.1, and reT-3 cells. *GAPDH* is an internal control for PCRs.

(C–E) Quantitative PCR to compare the expression of major cell surface molecules (C), cell lytic molecules (D), and transcription factors and signal-transduction molecules (E) among PB CD4$^+$, PB CD8$^+$, reT-2.1, and H25-#4 cells. Individual PCR reactions were normalized against 18S rRNA.

(F and G) Global gene expression was analyzed using a cDNA microarray. Heat maps show the correlation coefficients between samples (F) and differential expression (>3-fold) of genes relative to NK cells (G). Red and green colorations indicate increased and decreased expression, respectively.

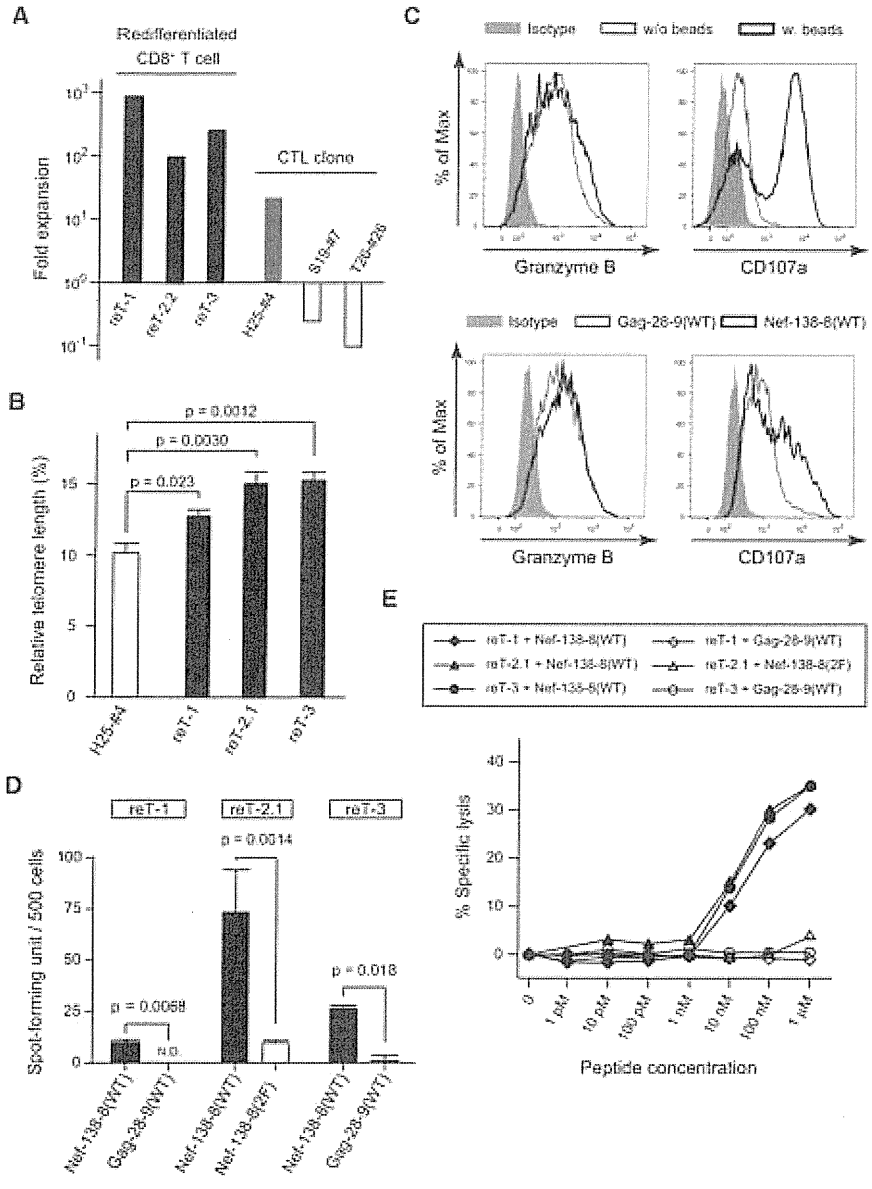

Figure 4. Redifferentiated T Cells Show T Cell Functionality and the Same Antigen Specificity as the Original CTL Clone

(A) Expansion ratios for reT-1, reT-2.2, and reT-3 cells elicited by PHA, IL-7, and IL-15 stimulation for 2 weeks. H25-#4 is the original clone. S19-#7 and T26-#26 were other Nef-138-8(WT)-specific CTL clones derived from different patients.

(B) Relative telomere length determined using flow-FISH. Data are presented as mean ± SEM.

(C) Intracellular production of granzyme B (left panel) and CD107a mobilization (right panel) induced by stimulation of reT-2.1 cells with α-CD3/CD28 beads or Nef-138-8(WT). Shaded plot: stimulated cells, isotype antibody; gray line: unstimulated cells, granzyme B or CD107a antibody; black line: stimulated cells, granzyme B or CD107a antibody.

(D) IFN-γ production in the presence of Nef-138-8(WT) measured using ELISPOT. Data are presented as mean ± SD. N.D., not determined.

(E) Standard ^{51}Cr release assay performed using the indicated concentrations of Nef-138-8(WT). Effector:target = 5:1.

See Figure S6 for additional data.

"rejuvenation." Throughout the experiments, neither autonomous cell expansion nor aberrant cell survival without cytokines as leukemia cells was observed (data not shown). Taken together, these data indicate that by passing through the T-iPSC state, cloned cytotoxic T cells can become "rejuvenated" to central memory-like T cells with excellent potential for proliferation and survival.

Redifferentiated CD8$^+$ T Cells Exhibit Antigen-Specific T Cell Functionality

To determine whether redifferentiated CD8$^+$ T cells exerted cytotoxic effects upon recognition of specific peptides in the context of an MHC, we performed functional assays using HLA-A24-positive B-LCL cells as antigen-presenting cells. Gag-28-9(WT) (KYKLKHIVW) is an antigenic peptide (aa 28–36) from the HIV-1 Gag protein (Altfeld et al., 2006), whereas Nef-138-8(2F) (RFPLTFGW) is a Tyr-to-Phe-substituted single-residue mutant form of Nef-138-8(WT). Both peptides were presented on HLA-A24 cells.

One of the major mechanisms by which CTLs induce cytotoxity is the secretion of cytolytic molecules triggered by TCR signaling. Intracellular staining revealed that the cytolytic molecule granzyme B was produced and stored in the granules of redifferentiated CD8$^+$ T cells (Figure 4C, left column). CD107a, also known as lysosomal-associated membrane protein 1 (LAMP1), is a granulocyte membrane protein that transiently appears at the cell surface and is coupled to degranulation (secretion of cytolytic molecules) of the stimulated CTLs, after which CD107a returns to the cytoplasm (Rubio et al., 2003). CD107a molecules on the cell surface were captured by a fluorochrome-conjugated antibody when redifferentiated CD8$^+$ T cells were stimulated with α-CD3/28 beads or Nef-138-8(WT) peptide, but not in the absence of the beads or Gag-28-9(WT) peptide (Figure 4C, right column). In the second experiment, we used the enzyme-linked immunosorbent spot (ELISPOT) assay to assess cytokine productivity per cell and confirmed that redifferentiated CD8$^+$ T cells produced significant levels of IFN-γ in response to stimulation by its specific antigen, Nef-138-8(WT) (Figure 4D). In a separate experiment, we used a ^{51}Cr release assay to investigate cytolytic capacity and found that redifferentiated CD8$^+$ T cells lysed ^{51}Cr-incorporated B-LCLs only when Nef-138-8(WT) was presented on B-LCLs (Figure 4E).

These results are highly indicative that redifferentiated CD8$^+$ T cells can release cytotoxic molecules and kill antigen-expressing target cells in an antigen-specific manner. Moreover,

monoclonal TCRs mediate highly precise cell targeting that should broaden the therapeutic window for antigen-specific T cell therapy by avoiding the troublesome mispairing TCRs that can occur with the commonly used exogenous TCR transfer technique for inducing antigen-specific T cells from hematopoietic stem cells or peripheral mature T cells (Bendle et al., 2010; Brenner and Okur, 2009).

DISCUSSION

Using a HIV-1-epitope-specific CTL clone as a model, we demonstrated here that the reprogramming into pluripotency of a T cell clone and the subsequent redifferentiation to mature functional $CD8^+$ T cells are possible. These redifferentiated $CD8^+$ T cells are highly proliferative naive cells with elongated telomeres, and they exert T cell functions in the same HIV-1-epitope-specific manner, permitting the inference that this process of reprogramming and redifferentiation can rejuvenate mature antigen-specific T cells.

Generation of iPSCs from T cells was initially difficult. On the basis of reports by Seki et al. (2010), we also found that SeV is suitable for the reprogramming of aged and exhausted fibroblasts, as well as of T cells. We also found that coexpression of SV40 large T antigen acted synergistically with the classic Yamanaka factors in enhancing the reprogramming efficiency of T cells. Therefore, SV40 large-T antigen introduction using the SeV vector system was also included in the protocol. Worth noting is that c-*MYC* is a known oncogene, and when it is inserted into the genomic DNA by the retroviral vector, it may become a risk for tumorigenesis in the generation of iPSCs. The same concern does not apply to SeV vector systems, given that the genomic RNA could be removed from the cytosol after reprogramming. Therefore, the utilization of SeV vectors both improved reprogramming efficiency and shielded redifferentiating cells from oncogene- or provirus-mediated tumorigenesis (Kohn et al., 2003).

In the redifferentiation experiments, mimicking TCR signaling led to CD8-linage specification without reassembly of *TCRA* genes. Preassembled TCR genes are a distinctive feature of T-iPSCs not found on other pluripotent stem cells. TCR$\alpha\beta$ is aberrantly expressed on redifferentiating CD4/CD8 DN cells, and the TCR signaling evoked results in the cessation of *RAG* expression. Serwold and colleagues reported that aberrantly early expression of TCR from preassembled *Tcra* and *Tcrb* following TCR signaling in murine thymocytes drives later lymphomagenesis (Serwold et al., 2010). They cautioned that T-iPSCs might confer risk for TCR-mediated lymphomagenesis. Therefore, the redifferentiation method will need to be further optimized and confirmed for clinical safety before application in practical treatments. This may be achieved by the use of an inducible suicide-gene system for eliminating unwanted tumors after injections (Hara et al., 2008; Veldwijk et al., 2004).

Immunological assays found that the redifferentiated $CD8^+$ T cells exerted T cell functions such as cytolytic activity, IFN-γ secretion, and degranulation in a normal manner when stimulated with their specific antigens. The most striking difference was in their proliferation capacity and elongated telomeres, which correlates with the central-memory T cell phenotype. Stem cell-like memory T cells (T_{SCM}) were recently identified as a subpopulation of T cells that has the capacity for self-renewal and that is multipotent and able to generate central memory, effector memory, and effector T cells (Gattinoni et al., 2011; Turtle et al., 2009). In a humanized mouse model, T_{SCM} cells reconstituted the T cell population more efficiently than other known memory subsets while mediating a superior antitumor response. It was found that inhibition of GSK3β enhances the generation of T_{SCM} in culture. Combining T-iPSC-mediated T cell rejuvenation with GSK3β inhibition may therefore enable efficient generation of T_{SCM} cells and permit highly effective immunotherapy along with the reconstitution of a normal T cell immune system.

Although these data suggest that rejuvenated T cells enjoy an advantage over the original T cell clone, it remains unclear whether these HIV-epitope-specific rejuvenated T cells are effective in improving the overall status of HIV infection. This is because the role of $CD8^+$ T cells in HIV infection appears to vary depending on the disease stage (Appay et al., 2000; Borrow et al., 1994; Brodie et al., 1999; Day et al., 2006; Koup et al., 1994). Evasion of the immune response through CTL escape is another important factor in HIV pathogenesis, and the escaped virus is a substantial hurdle for HIV therapies (Phillips et al., 1991). Therefore, this system may work best instead against tumors such as a melanoma, for which certain antigenic epitopes are known, or against viral infections other than HIV, for which the roles of $CD8^+$ cytotoxic T cells are more established. Nonetheless, the system described in our study will make it possible to preserve and to supply highly proliferative, functional $CD8^+$ T cells specific to a variety of HIV epitopes without worrying about exhaustion. It may also act as a valuable tool in better understanding the role of adoptive immunity in HIV infection.

Here, we have presented a proof of concept of $CD8^+$ T cell rejuvenation. The concept is not limited only to $CD8^+$ cytotoxic T cells. It may also be applied to $CD4^+$ helper or regulatory T cells to control desired or undesired immune reactions in the context of malignancies, chronic viral infections, autoimmune diseases, or transplantation-related immune disorders, if optimization of redifferentiation conditions can be achieved. Biological and technical challenges lie ahead, but the data presented in this work open new avenues toward antigen-specific T cell therapies that will supply unlimited numbers of rejuvenated T cells and will regenerate patients' immune systems.

EXPERIMENTAL PROCEDURES

Generation of Antigen-Specific CTL Clones

Nef138-8(WT)-specific CTL lines were induced from PBMCs of a patient chronically infected with HIV-1 who is positive for HLA-A24, as described (Kawana-Tachikawa et al., 2002). Each CTL line was expanded from a single-cell sorted tetramer$^+$ T cell, and the cells in every CTL line were confirmed for expression of only one kind of TCR$\alpha\beta$. For more details of CTL-clone establishment, see the Supplemental Experimental Procedures.

Generation of T-iPSCs

Human iPSCs were established from PB T cells or a CTL clone as described (Takayama et al., 2010), slightly modifying the culture conditions. In brief, T cells were stimulated by α-CD3/CD28 antibody-coated beads (Miltenyi Biotec) or by 5 μg/ml PHA-L (Sigma-Aldrich). The activated cells were transduced with reprogramming factors via retroviral or SeV vectors and were cultured in RH10 medium (RPMI-1640 supplemented with 10% human AB Serum, 2 mM L-glutamine, 100 U/ml penicillin, and 100 ng/ml streptomycin), which was

gradually replaced with human iPSC medium (Dulbecco's modified Eagle's medium/F12 FAM supplemented with 20% knockout serum replacer, 2 mM L-glutamine, 1% nonessential amino acids, 10 μM 2-mercaptoethanol, and 5 ng/ml basic fibroblast growth factor [bFGF]). The established iPSC clones were transfected with small interfering RNA L527 (Nishimura et al., 2011) using Lipofectamine RNAi Max (Invitrogen) for removal of SeV vectors from the cytoplasm.

Analysis of TCR Gene Rearrangement in Genomic DNA

Genomic DNA was extracted from approximately 5×10^6 cells using QIAamp DNA kits (QIAGEN) according to the manufacturer's instructions. For *TCRB* gene rearrangement analysis, PCR was performed according to BIOMED-2 protocols (van Dongen et al., 2003). For *TCRA* gene rearrangement analysis, PCR was performed using the primers shown in Figure S2 and LA Taq HS (TaKaRa). The PCR protocol entailed three amplification cycles (30 s at 95°C, 45 s at 68°C, and 6 min at 72°C); 15 amplification cycles (30 s at 95°C, 45 s at 62°C, and 6 min at 72°C); and 12 amplification cycles (15 s at 95°C, 30 s at 62°C, and 6 min at 72°C). The dominant band within the expected size range was purified using a QIAquick gel-extraction kit (QIAGEN) and was then sequenced. V, D, and J segment usages were identified by comparison to the ImMunoGeneTics (IMGT) database (http://www.imgt.org/) and by using an online tool (IMGT/V-QUEST) (Lefranc, 2003). Gene-segment nomenclature follows IMGT usage.

Analysis of TCR Gene Rearrangement in mRNA

A method based on the "switch mechanism at the 5'-end of the reverse transcript (SMART)" (Du et al., 2006) was used to synthesize double-stranded cDNAs (Super SMART cDNA synthesis kit; BD Clontech). Reverse transcription was conducted with the 3' SMART CDS primer, SMART II A oligonucleotides (Super SMART cDNA synthesis kit), and PrimeScript Reverse Transcriptase (TaKaRa) for 90 min at 42°C. Double-stranded cDNA was then synthesized and was amplified with 5' PCR Primer II A (Super SMART cDNA synthesis kit), and reagents were provided in an Advantage 2 PCR Kit (BD Clontech). The PCR protocol entailed 20 cycles of 5 s at 95°C, 5 s at 65°C, and 3 min at 68°C. The amplified double-stranded cDNA was used as templates in TCRA- or TCRB-specific amplification reactions. With forward primer (2^{nd}_5'-SMART) and reverse primer (3'-TRAC for *TCRA* or 3'-TRBC for *TCRB*), 25 cycles of amplification were performed (30 s at 94°C, 30 s at 55°C, and 1 min at 72°C). PCR products were cloned into pGEM-T Easy Vector (Promega) and were sequenced.

T Cell Differentiation from T-iPSCs

To differentiate human iPSCs into hematopoietic cells, we slightly modified a previously described protocol (Takayama et al., 2008). Small clumps of iPSCs (<100 cells) were transferred onto irradiated C3H10T1/2 cells and co-cultured in EB medium (Iscove's modified Dulbecco's medium supplemented with 15% fetal bovine serum [FBS] and a cocktail of 10 μg/ml human insulin, 5.5 μg/ml human transferrin, 5 ng/ml sodium selenite, 2 mM L-glutamine, 0.45 mM α-monothioglycerol, and 50 μg/ml ascorbic acid) in the presence of VEGF, SCF, and FLT-3L. Hematopoietic cells contained in iPSC sacs were collected and were transferred onto irradiated OP9-DL1 cells (provided by RIKEN BRC through the National BioResource Project of the Ministry of Education, Culture, Sports, Science, and Technology [MEXT]) (Watarai et al., 2010). The hematopoietic cells underwent T lineage differentiation on OP9-DL1 cells during coculture in OP9 medium (αMEM supplemented with 15% FBS, 2 mM L-glutamine, 100 U/ml penicillin, and 100 ng/ml streptomycin) in the presence of FLT-3L and IL-7. The T lineage cells were then harvested, mixed with irradiated HLA-A24$^+$ PBMCs, and cocultured in RH10 medium in the presence of IL-7 and IL-15.

Intracellular Staining

For intracellular staining of granzyme B, T cells were stimulated by α-CD3/28 beads or peptide-loaded HLA-A24$^+$ B-LCLs. After 2 hr, brefeldin A (5 μg/ml; Invitrogen) was added, with incubation for 4 hours more. Cells were then harvested and fixed in Fixation/Permeabilization solution (BD Biosciences). Intracellular staining was performed as per the manufacturer's protocol using Perm/Wash buffer (BD Biosciences) and fluorescein isothiocyanate (FITC)-conjugated granzyme B antibody (BD Biosciences). For capturing CD107a transiently expressed on cell surfaces, T cells were incubated with α-CD3/28 beads or peptide-loaded HLA-A24$^+$ B-LCLs and were cultured with FITC-conjugated CD107a antibody (BioLegend) for 6 hr. Harvested cells were fixed and stained as described above. Data were acquired on FACSAria II equipment (BD Biosciences) and analyzed using FlowJo software (Tree Star).

Measurement of Telomere Length by Flow-FISH

Telomere length was measured using a Telomere PNA Kit/FITC (DAKO) as previously described (Neuber et al., 2003).

ELISPOT and ^{51}Cr Release Assays

The antigen-specific responses of T cells were measured using an ELISPOT assay for IFN-γ and a standard ^{51}Cr release assay as described (Kawana-Tachikawa et al., 2002; Tsunetsugu-Yokota et al., 2003). HLA-A24$^+$ B-LCLs were used as antigen-presenting cells.

Statistics

All data are presented as mean ± SD. All statistics were performed using Excel (Microsoft) and Prism (GraphPad software) programs, applying two-tailed Student's t test. Values of $p < 0.05$ were considered significant. For additional details, see the Supplemental Experimental Procedures.

ACCESSION NUMBERS

The Gene Expression Omnibus accession number for microarray data reported in this paper is GSE43136.

SUPPLEMENTAL INFORMATION

Supplemental Information includes six figures, three tables, and Supplemental Experimental Procedures and can be found with this article online at http://dx.doi.org/10.1016/j.stem.2012.11.002.

ACKNOWLEDGMENTS

We thank Yumiko Ishii and Yuji Yamazaki (The University of Tokyo) for FACS operation; Sou Nakamura, Ryoko Jono-Onishi, and Shuichi Kitayama (The University of Tokyo) for technical help; Hiroshi Kawamoto, Kyoko Masuda, and Raul Vizcardo (RIKEN Center for Allergy and Immunology) for kindly providing OP9-DL1 cells and for helpful discussions; Yasuharu Nishimura and Satoru Senju (Kumamoto University) for kindly providing T cell clones; Makoto Otsu, Akihide Kamiya, Motoo Watanabe, Ayako Kamisato, and Masataka Kasai (The University of Tokyo) and Masaki Yasukawa, Hiroshi Fujiwara, and Toshiki Ochi (Ehime University) for helpful discussions; and Alex Knisely and Huan-Ting Lin for critical reading of the manuscript. The project was supported in part by a grant from the Project for Realization of Regenerative Medicine, by a Grant-in-Aid for Scientific Research (KAKENHI) and by the Global Center of Excellence program from MEXT of Japan, by a Grant-in-Aid for scientific research from the Japan Society for the Promotion of Science, and by grants for AIDS research from the Ministry of Health, Labor, and Welfare of Japan. The experimental protocol was approved by the institutional regulation board for human ethics at the Institute of Medical Science, University of Tokyo (approval number: 20-6-0826). The entire study was conducted in accordance with the Declaration of Helsinki.

Received: May 31, 2012
Revised: September 28, 2012
Accepted: November 6, 2012
Published: January 3, 2013

REFERENCES

Alt, F.W., and Baltimore, D. (1982). Joining of immunoglobulin heavy chain gene segments: implications from a chromosome with evidence of three D-JH fusions. Proc. Natl. Acad. Sci. USA *79*, 4118–4122.

Altfeld, M., Kalife, E.T., Qi, Y., Streeck, H., Lichterfeld, M., Johnston, M.N., Burgett, N., Swartz, M.E., Yang, A., Alter, G., et al. (2006). HLA Alleles

Associated with Delayed Progression to AIDS Contribute Strongly to the Initial CD8(+) T Cell Response against HIV-1. PLoS Med. *3*, e403.

Appay, V., Nixon, D.F., Donahoe, S.M., Gillespie, G.M., Dong, T., King, A., Ogg, G.S., Spiegel, H.M., Conlon, C., Spina, C.A., et al. (2000). HIV-specific CD8(+) T cells produce antiviral cytokines but are impaired in cytolytic function. J. Exp. Med. *192*, 63–75.

Bendle, G.M., Linnemann, C., Hooijkaas, A.I., Bies, L., de Witte, M.A., Jorritsma, A., Kaiser, A.D., Pouw, N., Debets, R., Kieback, E., et al. (2010). Lethal graft-versus-host disease in mouse models of T cell receptor gene therapy. Nat. Med. *16*, 565–570, 1p following 570.

Borgulya, P., Kishi, H., Uematsu, Y., and von Boehmer, H. (1992). Exclusion and inclusion of alpha and beta T cell receptor alleles. Cell *69*, 529–537.

Borrow, P., Lewicki, H., Hahn, B.H., Shaw, G.M., and Oldstone, M.B. (1994). Virus-specific CD8+ cytotoxic T-lymphocyte activity associated with control of viremia in primary human immunodeficiency virus type 1 infection. J. Virol. *68*, 6103–6110.

Brenner, M.K., and Okur, F.V. (2009). Overview of gene therapy clinical progress including cancer treatment with gene-modified T cells. Hematology (Am. Soc. Hematol. Educ. Program), 675–681.

Brivanlou, A.H., Gage, F.H., Jaenisch, R., Jessell, T., Melton, D., and Rossant, J. (2003). Stem cells. Setting standards for human embryonic stem cells. Science *300*, 913–916.

Brodie, S.J., Lewinsohn, D.A., Patterson, B.K., Jiyamapa, D., Krieger, J., Corey, L., Greenberg, P.D., and Riddell, S.R. (1999). In vivo migration and function of transferred HIV-1-specific cytotoxic T cells. Nat. Med. *5*, 34–41.

Brown, M.E., Rondon, E., Rajesh, D., Mack, A., Lewis, R., Feng, X., Zitur, L.J., Learish, R.D., and Nuwaysir, E.F. (2010). Derivation of induced pluripotent stem cells from human peripheral blood T lymphocytes. PLoS ONE *5*, e11373.

Butler, N.S., Nolz, J.C., and Harty, J.T. (2011). Immunologic considerations for generating memory CD8 T cells through vaccination. Cell. Microbiol. *13*, 925–933.

Day, C.L., Kaufmann, D.E., Kiepiela, P., Brown, J.A., Moodley, E.S., Reddy, S., Mackey, E.W., Miller, J.D., Leslie, A.J., DePierres, C., et al. (2006). PD-1 expression on HIV-specific T cells is associated with T-cell exhaustion and disease progression. Nature *443*, 350–354.

Du, G., Qiu, L., Shen, L., Sehgal, P., Shen, Y., Huang, D., Letvin, N.L., and Chen, Z.W. (2006). Combined megaplex TCR isolation and SMART-based real-time quantitation methods for quantitating antigen-specific T cell clones in mycobacterial infection. J. Immunol. Methods *308*, 19–35.

Freberg, C.T., Dahl, J.A., Timoskainen, S., and Collas, P. (2007). Epigenetic reprogramming of OCT4 and NANOG regulatory regions by embryonal carcinoma cell extract. Mol. Biol. Cell *18*, 1543–1553.

Fusaki, N., Ban, H., Nishiyama, A., Saeki, K., and Hasegawa, M. (2009). Efficient induction of transgene-free human pluripotent stem cells using a vector based on Sendai virus, an RNA virus that does not integrate into the host genome. Proc. Jpn. Acad., Ser. B, Phys. Biol. Sci. *85*, 348–362.

Gattinoni, L., Lugli, E., Ji, Y., Pos, Z., Paulos, C.M., Quigley, M.F., Almeida, J.R., Gostick, E., Yu, Z., Carpenito, C., et al. (2011). A human memory T cell subset with stem cell-like properties. Nat. Med. *17*, 1290–1297.

Greenberg, P.D. (1991). Adoptive T cell therapy of tumors: mechanisms operative in the recognition and elimination of tumor cells. Adv. Immunol. *49*, 281–355.

Hanna, J., Markoulaki, S., Schorderet, P., Carey, B.W., Beard, C., Wernig, M., Creyghton, M.P., Steine, E.J., Cassady, J.P., Foreman, R., et al. (2008). Direct reprogramming of terminally differentiated mature B lymphocytes to pluripotency. Cell *133*, 250–264.

Hara, A., Aoki, H., Taguchi, A., Niwa, M., Yamada, Y., Kunisada, T., and Mori, H. (2008). Neuron-like differentiation and selective ablation of undifferentiated embryonic stem cells containing suicide gene with Oct-4 promoter. Stem Cells Dev. *17*, 619–627.

Hochedlinger, K., and Jaenisch, R. (2002). Monoclonal mice generated by nuclear transfer from mature B and T donor cells. Nature *415*, 1035–1038.

Huang, C., and Kanagawa, O. (2001). Ordered and coordinated rearrangement of the TCR alpha locus: role of secondary rearrangement in thymic selection. J. Immunol. *166*, 2597–2601.

Ikawa, T., Hirose, S., Masuda, K., Kakugawa, K., Satoh, R., Shibano-Satoh, A., Kominami, R., Katsura, Y., and Kawamoto, H. (2010). An essential developmental checkpoint for production of the T cell lineage. Science *329*, 93–96.

Jameson, S.C., and Masopust, D. (2009). Diversity in T cell memory: an embarrassment of riches. Immunity *31*, 859–871.

June, C.H. (2007). Adoptive T cell therapy for cancer in the clinic. J. Clin. Invest. *117*, 1466–1476.

Kaneko, S., Mastaglio, S., Bondanza, A., Ponzoni, M., Sanvito, F., Aldrighetti, L., Radrizzani, M., La Seta-Catamancio, S., Provasi, E., Mondino, A., et al. (2009). IL-7 and IL-15 allow the generation of suicide gene-modified alloreactive self-renewing central memory human T lymphocytes. Blood *113*, 1006–1015.

Kawana-Tachikawa, A., Tomizawa, M., Nunoya, J., Shioda, T., Kato, A., Nakayama, E.E., Nakamura, T., Nagai, Y., and Iwamoto, A. (2002). An efficient and versatile mammalian viral vector system for major histocompatibility complex class I/peptide complexes. J. Virol. *76*, 11982–11988.

Khor, B., and Sleckman, B.P. (2002). Allelic exclusion at the TCRbeta locus. Curr. Opin. Immunol. *14*, 230–234.

Klebanoff, C.A., Gattinoni, L., and Restifo, N.P. (2006). CD8+ T-cell memory in tumor immunology and immunotherapy. Immunol. Rev. *211*, 214–224.

Kohn, D.B., Sadelain, M., and Glorioso, J.C. (2003). Occurrence of leukaemia following gene therapy of X-linked SCID. Nat. Rev. Cancer *3*, 477–488.

Koup, R.A., Safrit, J.T., Cao, Y., Andrews, C.A., McLeod, G., Borkowsky, W., Farthing, C., and Ho, D.D. (1994). Temporal association of cellular immune responses with the initial control of viremia in primary human immunodeficiency virus type 1 syndrome. J. Virol. *68*, 4650–4655.

Krangel, M.S. (2009). Mechanics of T cell receptor gene rearrangement. Curr. Opin. Immunol. *21*, 133–139.

Lafaille, J.J., DeCloux, A., Bonneville, M., Takagaki, Y., and Tonegawa, S. (1989). Junctional sequences of T cell receptor gamma delta genes: implications for gamma delta T cell lineages and for a novel intermediate of V-(D)-J joining. Cell *59*, 859–870.

Lefranc, M.P. (2003). IMGT databases, web resources and tools for immunoglobulin and T cell receptor sequence analysis, http://imgt.cines.fr. Leukemia *17*, 260–266.

Loh, Y.H., Hartung, O., Li, H., Guo, C., Sahalie, J.M., Manos, P.D., Urbach, A., Heffner, G.C., Grskovic, M., Vigneault, F., et al. (2010). Reprogramming of T cells from human peripheral blood. Cell Stem Cell *7*, 15–19.

Lu, P.H., and Negrin, R.S. (1994). A novel population of expanded human CD3+CD56+ cells derived from T cells with potent in vivo antitumor activity in mice with severe combined immunodeficiency. J. Immunol. *153*, 1687–1696.

MacLeod, M.K., Kappler, J.W., and Marrack, P. (2010). Memory CD4 T cells: generation, reactivation and re-assignment. Immunology *130*, 10–15.

Marion, R.M., Strati, K., Li, H., Tejera, A., Schoeftner, S., Ortega, S., Serrano, M., and Blasco, M.A. (2009). Telomeres acquire embryonic stem cell characteristics in induced pluripotent stem cells. Cell Stem Cell *4*, 141–154.

Monteiro, J., Batliwalla, F., Ostrer, H., and Gregersen, P.K. (1996). Shortened telomeres in clonally expanded CD28-CD8+ T cells imply a replicative history that is distinct from their CD28+CD8+ counterparts. J. Immunol. *156*, 3587–3590.

Morgan, R.A., Dudley, M.E., Wunderlich, J.R., Hughes, M.S., Yang, J.C., Sherry, R.M., Royal, R.E., Topalian, S.L., Kammula, U.S., Restifo, N.P., et al. (2006). Cancer regression in patients after transfer of genetically engineered lymphocytes. Science *314*, 126–129.

Neuber, K., Schmidt, S., and Mensch, A. (2003). Telomere length measurement and determination of immunosenescence-related markers (CD28, CD45RO, CD45RA, interferon-gamma and interleukin-4) in skin-homing T cells expressing the cutaneous lymphocyte antigen: indication of a non-ageing T-cell subset. Immunology *109*, 24–31.

Nishimura, K., Sano, M., Ohtaka, M., Furuta, B., Umemura, Y., Nakajima, Y., Ikehara, Y., Kobayashi, T., Segawa, H., Takayasu, S., et al. (2011). Development of defective and persistent Sendai virus vector: a unique gene delivery/expression system ideal for cell reprogramming. J. Biol. Chem. *286*, 4760–4771.

Padovan, E., Casorati, G., Dellabona, P., Meyer, S., Brockhaus, M., and Lanzavecchia, A. (1993). Expression of two T cell receptor alpha chains: dual receptor T cells. Science *262*, 422–424.

Petrie, H.T., Livak, F., Schatz, D.G., Strasser, A., Crispe, I.N., and Shortman, K. (1993). Multiple rearrangements in T cell receptor alpha chain genes maximize the production of useful thymocytes. J. Exp. Med. *178*, 615–622.

Phillips, R.E., Rowland-Jones, S., Nixon, D.F., Gotch, F.M., Edwards, J.P., Ogunlesi, A.O., Elvin, J.G., Rothbard, J.A., Bangham, C.R., Rizza, C.R., et al. (1991). Human immunodeficiency virus genetic variation that can escape cytotoxic T cell recognition. Nature *354*, 453–459.

Porter, D.L., Levine, B.L., Kalos, M., Bagg, A., and June, C.H. (2011). Chimeric antigen receptor-modified T cells in chronic lymphoid leukemia. N. Engl. J. Med. *365*, 725–733.

Prlic, M., Lefrancois, L., and Jameson, S.C. (2002). Multiple choices: regulation of memory CD8 T cell generation and homeostasis by interleukin (IL)-7 and IL-15. J. Exp. Med. *195*, F49–F52.

Romero, P., Zippelius, A., Kurth, I., Pittet, M.J., Touvrey, C., Iancu, E.M., Corthesy, P., Devevre, E., Speiser, D.E., and Rufer, N. (2007). Four functionally distinct populations of human effector-memory CD8+ T lymphocytes. J. Immunol. *178*, 4112–4119.

Rubio, V., Stuge, T.B., Singh, N., Betts, M.R., Weber, J.S., Roederer, M., and Lee, P.P. (2003). Ex vivo identification, isolation and analysis of tumor-cytolytic T cells. Nat. Med. *9*, 1377–1382.

Seki, T., Yuasa, S., Oda, M., Egashira, T., Yae, K., Kusumoto, D., Nakata, H., Tohyama, S., Hashimoto, H., Kodaira, M., et al. (2010). Generation of induced pluripotent stem cells from human terminally differentiated circulating T cells. Cell Stem Cell *7*, 11–14.

Serwold, T., Hochedlinger, K., Inlay, M.A., Jaenisch, R., and Weissman, I.L. (2007). Early TCR expression and aberrant T cell development in mice with endogenous prerearranged T cell receptor genes. J. Immunol. *179*, 928–938.

Serwold, T., Hochedlinger, K., Swindle, J., Hedgpeth, J., Jaenisch, R., and Weissman, I.L. (2010). T-cell receptor-driven lymphomagenesis in mice derived from a reprogrammed T cell. Proc. Natl. Acad. Sci. USA *107*, 18939–18943.

Staerk, J., Dawlaty, M.M., Gao, Q., Maetzel, D., Hanna, J., Sommer, C.A., Mostoslavsky, G., and Jaenisch, R. (2010). Reprogramming of human peripheral blood cells to induced pluripotent stem cells. Cell Stem Cell *7*, 20–24.

Takahashi, K., Tanabe, K., Ohnuki, M., Narita, M., Ichisaka, T., Tomoda, K., and Yamanaka, S. (2007). Induction of pluripotent stem cells from adult human fibroblasts by defined factors. Cell *131*, 861–872.

Takayama, N., Nishikii, H., Usui, J., Tsukui, H., Sawaguchi, A., Hiroyama, T., Eto, K., and Nakauchi, H. (2008). Generation of functional platelets from human embryonic stem cells in vitro via ES-sacs, VEGF-promoted structures that concentrate hematopoietic progenitors. Blood *111*, 5298–5306.

Takayama, N., Nishimura, S., Nakamura, S., Shimizu, T., Ohnishi, R., Endo, H., Yamaguchi, T., Otsu, M., Nishimura, K., Nakanishi, M., et al. (2010). Transient activation of c-MYC expression is critical for efficient platelet generation from human induced pluripotent stem cells. J. Exp. Med. *207*, 2817–2830.

Tan, J.T., Ernst, B., Kieper, W.C., LeRoy, E., Sprent, J., and Surh, C.D. (2002). Interleukin (IL)-15 and IL-7 jointly regulate homeostatic proliferation of memory phenotype CD8+ cells but are not required for memory phenotype CD4+ cells. J. Exp. Med. *195*, 1523–1532.

Timmermans, F., Velghe, I., Vanwalleghem, L., De Smedt, M., Van Coppernolle, S., Taghon, T., Moore, H.D., Leclercq, G., Langerak, A.W., Kerre, T., et al. (2009). Generation of T cells from human embryonic stem cell-derived hematopoietic zones. J. Immunol. *182*, 6879–6888.

Tsunetsugu-Yokota, Y., Morikawa, Y., Isogai, M., Kawana-Tachikawa, A., Odawara, T., Nakamura, T., Grassi, F., Autran, B., and Iwamoto, A. (2003). Yeast-derived human immunodeficiency virus type 1 p55(gag) virus-like particles activate dendritic cells (DCs) and induce perforin expression in Gag-specific CD8(+) T cells by cross-presentation of DCs. J. Virol. *77*, 10250–10259.

Turka, L.A., Schatz, D.G., Oettinger, M.A., Chun, J.J., Gorka, C., Lee, K., McCormack, W.T., and Thompson, C.B. (1991). Thymocyte expression of RAG-1 and RAG-2: termination by T cell receptor cross-linking. Science *253*, 778–781.

Turtle, C.J., Swanson, H.M., Fujii, N., Estey, E.H., and Riddell, S.R. (2009). A distinct subset of self-renewing human memory CD8+ T cells survives cytotoxic chemotherapy. Immunity *31*, 834–844.

van Dongen, J.J., Langerak, A.W., Brüggemann, M., Evans, P.A., Hummel, M., Lavender, F.L., Delabesse, E., Davi, F., Schuuring, E., Garcia-Sanz, R., et al. (2003). Design and standardization of PCR primers and protocols for detection of clonal immunoglobulin and T-cell receptor gene recombinations in suspect lymphoproliferations: report of the BIOMED-2 Concerted Action BMH4-CT98-3936. Leukemia *17*, 2257–2317.

Veldwijk, M.R., Berlinghoff, S., Laufs, S., Hengge, U.R., Zeller, W.J., Wenz, F., and Fruehauf, S. (2004). Suicide gene therapy of sarcoma cell lines using recombinant adeno-associated virus 2 vectors. Cancer Gene Ther. *11*, 577–584.

Virgin, H.W., Wherry, E.J., and Ahmed, R. (2009). Redefining chronic viral infection. Cell *138*, 30–50.

Vodyanik, M.A., Bork, J.A., Thomson, J.A., and Slukvin, I.I. (2005). Human embryonic stem cell-derived CD34+ cells: efficient production in the coculture with OP9 stromal cells and analysis of lymphohematopoietic potential. Blood *105*, 617–626.

von Boehmer, H. (2004). Selection of the T-cell repertoire: receptor-controlled checkpoints in T-cell development. Adv. Immunol. *84*, 201–238.

Watarai, H., Rybouchkin, A., Hongo, N., Nagata, Y., Sakata, S., Sekine, E., Dashtsoodol, N., Tashiro, T., Fujii, S., Shimizu, K., et al. (2010). Generation of functional NKT cells in vitro from embryonic stem cells bearing rearranged invariant Valpha14-Jalpha18 TCRalpha gene. Blood *115*, 230–237.

Weng, N.P., Hathcock, K.S., and Hodes, R.J. (1998). Regulation of telomere length and telomerase in T and B cells: a mechanism for maintaining replicative potential. Immunity *9*, 151–157.

Wherry, E.J. (2011). T cell exhaustion. Nat. Immunol. *12*, 492–499.

Zhang, N., and Bevan, M.J. (2011). CD8(+) T cells: foot soldiers of the immune system. Immunity *35*, 161–168.

Regular Article

HEMATOPOIESIS AND STEM CELLS

Role of SOX17 in hematopoietic development from human embryonic stem cells

Yaeko Nakajima-Takagi,[1,2] Mitsujiro Osawa,[1,2] Motohiko Oshima,[1,2] Haruna Takagi,[1] Satoru Miyagi,[1,2] Mitsuhiro Endoh,[2,3] Takaho A. Endo,[3,4] Naoya Takayama,[5,6] Koji Eto,[5,6] Tetsuro Toyoda,[4] Haruhiko Koseki,[2,3] Hiromitsu Nakauchi,[6] and Atsushi Iwama[1,2]

[1]Department of Cellular and Molecular Medicine, Graduate School of Medicine, Chiba University, Chiba, Japan; [2]JST, CREST, Tokyo, Japan; [3]RIKEN Research Center for Allergy and Immunology, Yokohama, Japan; [4]RIKEN Genomic Sciences Center, Yokohama, Japan; [5]Center for iPS Cell Research and Application, Kyoto University, Kyoto, Japan; and [6]Division of Stem Cell Therapy, Center for Stem Cell Biology and Regenerative Medicine, Institute of Medical Science, University of Tokyo, Tokyo, Japan

Key Points

- SOX17 plays a key role in priming hemogenic potential in endothelial cells during hematopoietic development from ES cells.

To search for genes that promote hematopoietic development from human embryonic stem cells (hESCs) and induced pluripotent stem cells (iPSCs), we overexpressed several known hematopoietic regulator genes in hESC/iPSC-derived CD34$^+$CD43$^-$ endothelial cells (ECs) enriched in hemogenic endothelium (HE). Among the genes tested, only *Sox17*, a gene encoding a transcription factor of the SOX family, promoted cell growth and supported expansion of CD34$^+$CD43$^+$CD45$^{-/low}$ cells expressing the HE marker VE-cadherin. *SOX17* was expressed at high levels in CD34$^+$CD43$^-$ ECs compared with low levels in CD34$^+$CD43$^+$CD45$^-$ pre-hematopoietic progenitor cells (pre-HPCs) and CD34$^+$CD43$^+$CD45$^+$ HPCs. *Sox17*-overexpressing cells formed semiadherent cell aggregates and generated few hematopoietic progenies. However, they retained hemogenic potential and gave rise to hematopoietic progenies on inactivation of Sox17. Global gene-expression analyses revealed that the CD34$^+$CD43$^+$CD45$^{-/low}$ cells expanded on overexpression of *Sox17* are HE-like cells developmentally placed between ECs and pre-HPCs. *Sox17* overexpression also reprogrammed both pre-HPCs and HPCs into HE-like cells. Genome-wide mapping of Sox17-binding sites revealed that Sox17 activates the transcription of key regulator genes for vasculogenesis, hematopoiesis, and erythrocyte differentiation directly. Depletion of *SOX17* in CD34$^+$CD43$^-$ ECs severely compromised their hemogenic activity. These findings suggest that SOX17 plays a key role in priming hemogenic potential in ECs, thereby regulating hematopoietic development from hESCs/iPSCs. (*Blood*. 2013;121(3):447-458)

Introduction

During mammalian development, 2 waves of hematopoiesis occur in sequential stages: first, a transient wave of primitive hematopoiesis, followed by definitive hematopoiesis. These stages are temporally and anatomically distinct and involve unique cellular and molecular regulators. The formation of primitive blood cells occurs early during fetal life, with coordinated progression from extraembryonic to intraembryonic sites of hematopoiesis. Within the embryo, definitive hematopoiesis undergoes developmentally stereotyped transitions; hematopoietic stem cells (HSCs) arising from the aorta-gonad-mesonephros region migrate first to the placenta and fetal liver and then to the spleen. Eventually, hematopoiesis shifts to the BM, where homeostatic blood formation is maintained postnatally.[1]

During definitive fetal hematopoiesis, HSCs emerge directly from a small population of endothelial cells (ECs) in the conceptus, referred to as the "hemogenic endothelium" (HE).[2-4] HE is located in all sites of HSC emergence, including the ventral aspect of the dorsal aorta, vitelline and umbilical arteries, yolk sac, and placenta. The process by which blood forms from HE involves an endothelial-to-hematopoietic cell transition during which individual cells bud out and detach from the endothelial layer.[2-4] HE is distinguished from all other ECs by the presence of a transcription factor called Runx1.[5] Runx1 is expressed in HE cells, in newly formed hematopoietic cell clusters, and in all functional HSCs.[6,7] A similar process occurs during hemangioblast differentiation in primitive blood cell formation. The extraembryonic yolk sac is considered to be the first site of emergence of the "hemangioblast," a mesodermal precursor with both endothelial and hematopoietic potential. Hemangioblasts differentiate into a HE intermediate, which gives rise to primitive hematopoietic cells but also definitive hematopoietic cells on activation of Runx1.[8]

Human embryonic stem cells (hESCs) and induced pluripotent stem cells (iPSCs) have been demonstrated to reproduce many aspects of embryonic hematopoiesis in stromal coculture or embryoid body (EB) culture. A recent study has provided evidence that hematopoietic differentiation of hESCs progresses through

Submitted May 19, 2012; accepted October 31, 2012. Prepublished online as *Blood* First Edition paper, November 20, 2012; DOI 10.1182/blood-2012-05-431403.

There is an Inside *Blood* commentary on this article in this issue.

The online version of this article contains a data supplement.

The publication costs of this article were defrayed in part by page charge payment. Therefore, and solely to indicate this fact, this article is hereby marked "advertisement" in accordance with 18 USC section 1734.

sequential stages: first is the HE, then primitive hematopoiesis, and finally definitive hematopoiesis, a process resembling the development of physiologic hematopoiesis.[9] However, the induction of hematopoietic cells from hESCs/iPSCs is still inefficient. Significant innovations are required before it will be possible to obtain sufficient numbers of the specific types of hematopoietic cells needed for therapeutic uses.

Sry-related high-mobility group box 17 (SOX17) is a member of the SOX family of DNA-binding transcription factors. Sox17 participates in various developmental processes and biologic activities, such as formation of definitive endoderm[10] and vascular development.[11] Moreover, recent studies have shown that Sox17 also plays an important role in fetal hematopoiesis in the yolk sac and fetal liver, especially in the maintenance of fetal and neonatal HSCs, but not adult HSCs.[12] Overexpression of *Sox17* has also been shown to confer fetal HSC characteristics onto adult hematopoietic progenitors.[13] Among SOX family members, Sox7, Sox17, and Sox18 are highly related and constitute the Sox subgroup F (SoxF). Sox7 and Sox18 are transiently expressed in hemangioblasts and hematopoietic precursors, respectively, at the onset of blood specification. Sustained expression of Sox7 and Sox18, but not Sox17, in early hematopoietic precursors from mouse ESCs and embryos enhances their proliferation while blocking their maturation.[14,15] However, the role of Sox17 in early hematopoietic development, particularly from hESCs, has not yet been clarified. In the present study, we tested the effect of overexpression of known hematopoietic regulator genes in hiPSC-derived $CD34^+CD43^-$ ECs enriched in HE to find genes that could be manipulated to efficiently produce hematopoietic cells from hESCs. We found that *Sox17* promotes the expansion of HE-like cells. We demonstrate that SOX17 functions in HE and plays a role in the development of hematopoietic cells from hESCs/iPSCs.

Methods

Cell lines

H1 hESCs (WiCell Research Institute) and TkCBV4-7 hiPSCs generated from human cord blood (CB) $CD34^+$ cells were maintained on irradiated murine embryonic fibroblasts in DMEM-F12 (Sigma-Aldrich) supplemented with 1× MEM nonessential amino acids (Gibco-Invitrogen), 1× GlutaMAX-I (Gibco-Invitrogen), 20% knockout serum replacement (Gibco-Invitrogen), 0.1mM 2-mercaptoethanol (Sigma-Aldrich), 1% penicillin/streptomycin solution (Sigma-Aldrich), and 5 ng/mL of human basic fibroblast growth factor (ReproCELL). Every 3-4 days, the cells were dissected into clumps of approximately 300-500 cells in a dissociation solution consisting of 0.25% trypsin, 20% knockout serum replacement, and 1mM $CaCl_2$ in PBS and transferred to a new feeder layer to maintain them in an undifferentiated state. The OP9 stromal cell line was kindly provided by Toru Nakano (Osaka University, Osaka, Japan). OP9 cells were maintained in α-MEM (Gibco-Invitrogen) supplemented with 2.2 g/L of sodium bicarbonate, 20% FBS, and 1% L-glutamine and penicillin/streptomycin solution (Sigma-Aldrich).

EB differentiation

H1 hESCs or TkCBV4-7 hiPSCs were dissociated into single cells with Accumax (Innovative Cell Technologies). The cells were washed with DMEM-F12 and recultured at 1×10^6 cells per 60-mm Petri dish (Falcon) in 5-mL mTeSR1 (StemCell Technologies) supplemented with 10μM LY27632 (Cayman), 2 ng/mL of human Bone Morphogenetic Protein 4 (BMP4; PeproTech), and 2 ng/mL of human activin A (PeproTech). At day 2 of culture, EBs were split from 1 60-mm Petri dish to 2 60-mm Petri dishes and cultured in EB medium consisting of IMDM (Sigma-Aldrich) containing 15% FBS, 1× GlutaMAX I, 1% penicillin/streptomycin solution, 200 μg/mL of bovine holo transferrin (Bovogen), 50 μg/mL of ascorbic acid (Sigma-Aldrich), and 450μM 1-thioglycerol (Sigma-Aldrich) supplemented with 2 ng/mL of human BMP4 and 5 ng/mL of human VEGF (PeproTech). At day 4 of culture, medium conditions were changed as described in Figure 1B. LY363947 (Cayman) was used as an inhibitor of TGFβ signaling. EBs were constantly cultured on a shaker at 70 rpm.

Flow cytometric analysis and OP9 coculture

EBs were dissociated with 0.25% trypsin-EDTA solution (Sigma-Aldrich) and filtered through a nylon screen to obtain a single-cell suspension. Flow cytometric analysis and cell sorting were performed using a FACSAria II cell sorter (BD Biosciences) and the data were analyzed using FlowJo Version 9.5.3 software (TreeStar). The following Abs were used for the flow cytometric analysis: CD34 (clone 581; Alexa Fluor 647 or PE-Cy7), CD43 (clone CD43-10G7; PE), CD45 (clone HI30; PE-Cy7), CD11b (clone M1/70; Brilliant Violet 421), CD235a (clone HIR2; PE), CD144 (VE-Cad; clone 16B1; PE), and CD309 (KDR; clone HKDR-1; APC). Sorted cells were resuspended in hematopoietic medium (IMDM, 10% FBS, 1% L-glutamine and penicillin/streptomycin solution) supplemented with 20 ng/mL of human SCF and 20 ng/mL of human thrombopoietin (TPO; PeproTech), and transferred onto semiconfluent irradiated OP9 cells. For mature hematopoietic cell differentiation, sorted cells were resuspended in HE medium supplemented with 20 ng/mL of SCF, 20 ng/mL of TPO, 10 ng/mL of human IL-3 (PeproTech), and 3 units/mL of human erythropoietin.

Retrovirus and lentivirus vectors, virus production, and transduction

Mouse *Sox17* fused to *ERT* with a 1× or 3× Flag tag was subcloned into the MIG retrovirus vector, which contains the long-terminal repeats from the murine stem cell virus and an internal ribosomal entry site upstream of the enhanced green fluorescent protein (GFP) as a marker gene. A recombinant vesicular stomatitis virus glycoprotein–pseudotyped high-titer retrovirus was generated using a 293gpg packaging cell line.[16] The virus containing media from the 293gpg cell cultures was concentrated by centrifugation at 6000*g* for 16 hours. To knock down *SOX17*, lentiviral vectors (CS-H1-shRNA-EF-1α-EGFP) expressing shRNA against human *SOX17* and *luciferase* were prepared. Target sequences were as follows; Sh-*SOX17*#1143; GCATGACTCCGGTGTGAAT, and Sh-*SOX17*#1273; GGCCAGAAGCAGTGTTACA. The viruses were produced as described previously.[17] EBs at approximately day 5-12 of culture were dissociated and the indicated cell populations were sorted using a FACSAria II. Sorted cells were seeded onto semiconfluent irradiated OP9 cells and transduced with a *SOX17-ERT* retrovirus or a *SOX17* knock-down virus. Transduced cells were cocultured with OP9 cells in the presence of the indicated cytokines. To induce nuclear translocation of SOX17-ERT, 4-hydroxy tamoxifen (4-OHT) was added to the medium to a concentration of 200nM on the following day.

Quantitative RT-PCR analysis

Total RNA was extracted using TRIzol reagent according to the manufacturer's instructions (Invitrogen). cDNA was synthesized from total RNA using ThermoScript RT-PCR System (Invitrogen). Quantitative RT-PCR was carried out using FastStart Universal Probe Master (Roche Applied Science), the Universal Probe Library (Roche Applied Science), and the Applied Biosystems 7300 Fast Real-Time PCR system (Applied Biosystems). Primer sequences and probe numbers used are listed in supplemental Methods (available on the *Blood* Web site; see the Supplemental Materials link at the top of the online article).

Colony-forming assay

Colony assays were performed in methylcellulose (StemCell Technologies) containing IMDM supplemented with 20 ng/mL of human SCF, 10 ng/mL of human IL-3, 10 ng/mL of human TPO, and 3 units/mL of human erythropoietin, and incubated at 37°C in a 5% CO_2 atmosphere. The colonies were counted at day 12 of culture. Images were captured by BIOREVO BZ-9000 (KEYENCE) with CFI Plan Fluor ELWD DM 20×C (Nikon) and processed using Adobe Photoshop Elements 4.0.

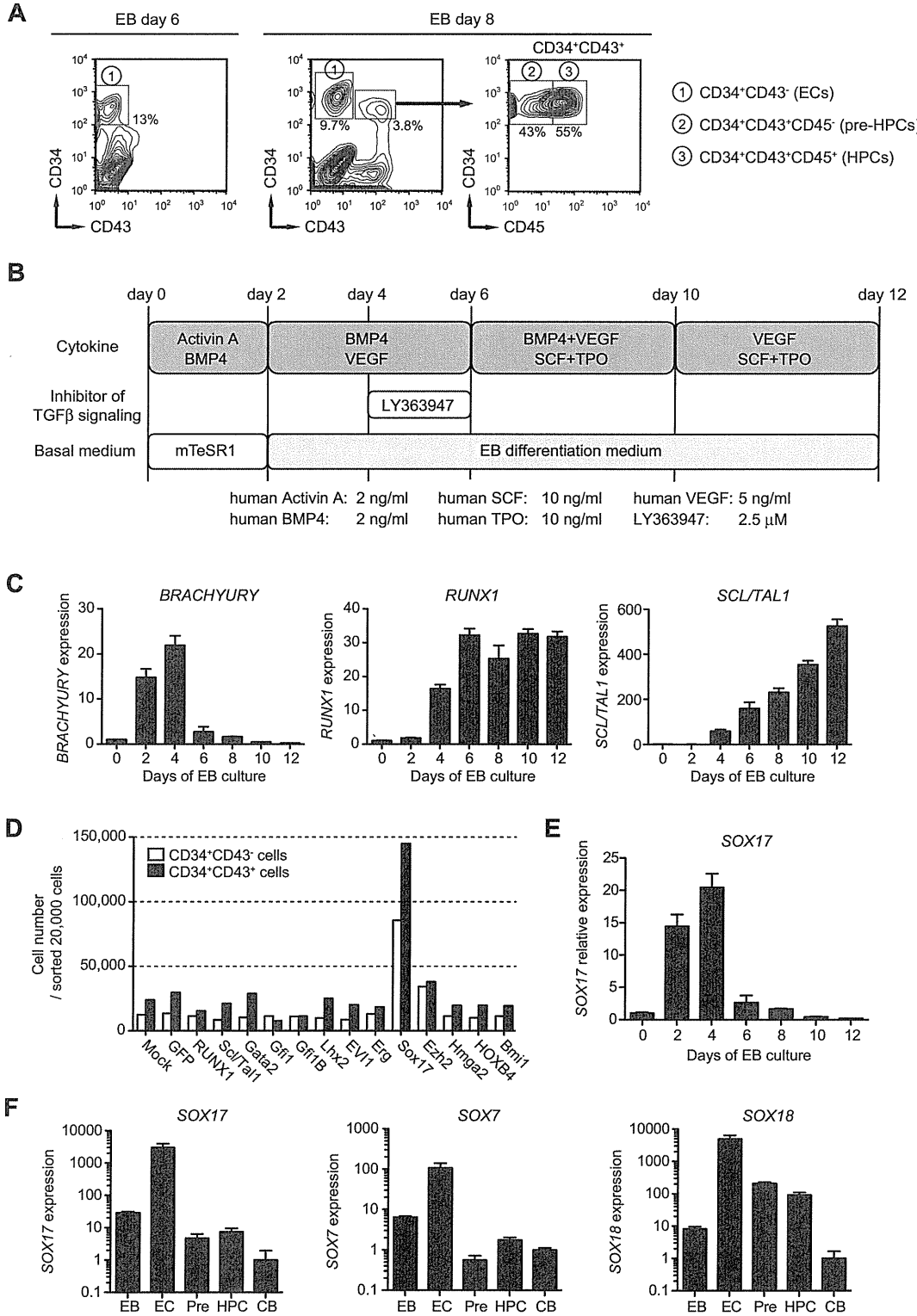

Figure 1. Screening of genes that promote expansion of hematopoietic cells from hESCs/hiPSCs. (A) Hematopoietic fractions derived from hESCs in EB culture used in this study. (B) Schematic representation of the protocol modified for efficient induction of pre-HPCs/HPCs from hESCs/hiPSCs in EB culture. (C) Expression of *BRACHYURY*, *RUNX1*, and *TAL1/SCL* expression during differentiation of hESCs in EBs determined by quantitative RT-PCR analysis. mRNA levels were normalized to *GAPDH* expression. Expression levels relative to that in hESCs (day 0 of EB culture) are shown as the means ± SD for triplicate analyses. (D) Cell growth of $CD34^+CD43^-$ cells from day 6 EBs and $CD34^+CD43^+$ cells from day 8 EBs. EBs were formed by suspension culture of hiPSCs. Sorted cells (2×10^4) were transduced with the indicated hematopoietic regulator genes and cultured on OP9 cells in the presence of 20 ng/mL of SCF and TPO. At day 14 of culture, the absolute numbers of cells were determined and are indicated in bars. Representative data from repeated experiments are shown. (E) Expression of *SOX17* during differentiation of hESCs in EBs determined by quantitative RT-PCR analysis. mRNA levels were normalized to *GAPDH* expression. Expression levels relative to that in hESCs (day 0 of EB culture) are shown as the means ± SD for triplicate analyses. (F) Expression of *SOX17*, *SOX7*, and *SOX18* in bulk EB cells, $CD34^+CD43^-$ cells (ECs), $CD34^+CD43^+CD45^-$ cells (pre-HPCs), and $CD34^+CD43^+CD45^+$ cells (HPCs) from day 8 EBs determined by quantitative RT-PCR analysis. mRNA levels were normalized to *GAPDH* expression. Expression levels relative to those in CB $CD34^+$ cells are shown as the means ± SD for triplicate analyses.

Gene-expression microarray

Total RNA was extracted using TRIzol reagent according to the manufacturer's instructions (Invitrogen). Purified total RNA was amplified and labeled using the WT expression kit (Ambion) according to the manufacturer's instructions. The labeled samples were hybridized to Human Promoter Gene 1.0 ST GeneChip arrays (Affymetrix) to assess and compare overall gene-expression profiles as described previously.[18] Microarray data were submitted to the Gene Expression Omnibus under accession number GSE38156. Expression profiles of the cells were clustered using hierarchical clustering. Distance between 2 samples was defined with the Pearson correlation using all or selected probes. Probes were selected using the Gene Ontology (GO) database or ChIP-on-chip data of Sox17.

ChIP-on-chip experiment

$CD34^+CD43^-$ cells from EBs at day 6 of culture were seeded on irradiated OP9 cells and transduced with a 3× Flag *SOX17-ERT* retrovirus. The cells were further cultured on OP9 cells in the presence of SCF, TPO (20 ng/mL), and 200nM 4-OHT. $CD34^+$ cells were collected at day 27 of culture by magnetic cell sorting using magnetic beads conjugated with anti-CD34 Abs (Miltenyi Biotec) and subjected to a ChIP assay using an anti-FLAG Ab (M2, Sigma). ChIP was carried out as described previously.[18] ChIP on chip analysis was carried out using the SurePrint G3 Human Promoter Kit, 1 × 1M (G4873A, Agilent Technologies). Purified immunoprecipitated and input DNA was subjected to T7 RNA polymerase-based amplification as described previously.[19] Labeling, hybridization, and washing were carried out according to the Agilent mammalian ChIP-on-chip protocol (Version 9.0). Scanned images were quantified with Agilent Feature Extraction software under standard conditions. The assignment of regions bound by SOX17 around transcription start sites (TSSs) was carried out using direct sequence alignment on the human genome database (National Center for Biotechnology Information Version 36). The location of SOX17-bound regions was compared with a set of transcripts derived from the MGI database. Bound regions that were within −8.0 kb to +4.0 kb of the TSS were assigned. Alignments on the human genome and TSSs of genes were retrieved from Ensembl (http://www.ensembl.org). Intensity ratios (IP/input: fold enrichment) were calculated, and the maximum value for each promoter region of a gene was used to represent the fold enrichment of the gene. Fold enrichment was calculated only for probes for which signals both from IP and input DNA were significant ($P < 10^{-3}$). ChIP-on-chip data were submitted to Gene Expression Omnibus under accession number GSE38156.

GO analysis

GO annotation was obtained using gene2go database (ftp://ftp.ncbi.nih.gov/gene/DATA/gene2go.gz) from Entrez (retrieved January 2012). Human genes were collected from the database and enrichment of SOX17-binding genes was distributed to 2 × 2 contingency tables for all GO terms (having/not having GO and binding/not binding to SOX17). We calculated P for each contingency table using hypergeometric distribution. The P value reflects the likelihood that we would observe the distribution by chance and significant GO terms were selected when $P < .001$.

Immunostaining

Sox17-ERT–transduced cells were sorted by flow cytometry and cultured on MAS-coated glass slides (Matsunami Glass Industries,) for 4 hours. The cells were then fixed with 2% paraformaldehyde and immunostained with an anti-laminin Ab (ab11575; Abcam) or an anti-FLAG Ab (M2; Sigma-Aldrich) for primary antibody reaction, and an Alexa Fluor 555 goat anti–rabbit IgG (Molecular Probes) or Alexa Fluor 555 goat anti–mouse IgG (Molecular Probes) for secondary antibody reaction, respectively. Images were captured by BIOREVO BZ-9000 (KEYENCE) with CFI Plan ApoVC 100×H (Nikon) and processed using Adobe Photoshop Elements 4.0.

Western blotting

Total cell lysate was resolved by SDS-PAGE and transferred to a PVDF membrane. The blots were probed with an anti-Sox17 Ab (09-038; Millipore) or an anti–α-tubulin (CP06; Calbiochem) and an HRP-conjugated secondary Ab. The protein bands were detected with Super-Signal West Pico Chemiluminescent Substrate (Thermo Scientific).

Results

Screening of genes that promote hematopoietic development from hESCs/iPSCs

Hematopoietic development from hESCs and hiPSCs recapitulates physiologic development, beginning in the conceptus and proceeding in a stepwise manner. $CD34^+CD43^-$ endothelial cells (ECs) enriched in HE give rise to the earliest hematopoietic progenitors, pre-hematopoietic progenitor cells (pre-HPCs) with an immunophenotype of $CD34^+CD43^+CD45^-$. Pre-HPCs then mature into $CD34^+CD43^+CD45^+$ HPCs that express CD45, a marker antigen specific to hematopoietic cells (Figure 1A).[20,21] We improved the conventional culture system to efficiently induce HPCs in EB culture by modifying cytokine conditions and adding an inhibitor of TGF-β signaling (Figure 1B). In our culture system, the expression of hematopoietic regulator genes such as *RUNX1* and *SCL/TAL1* increased in EBs after day 4 of culture accompanied by the decrease in expression of early mesodermal marker genes such as *Brachyury* (Figure 1C).

To identify genes that promote hematopoietic development from PSCs, we transduced hiPSC-derived ECs purified from day 6 EBs with several known hematopoietic regulator genes. We selected 13 genes that are known to play an important role in the development and/or maintenance of HSCs, including *RUNX1*, *Scl/Tal1*, *Gata2*, and *HOXB4*. The growth of the transduced cells was monitored in the presence of SCF and TPO for 14 days. Unexpectedly, most of these known regulator genes did not promote cell growth, but *Sox17* did. A similar effect was observed when we transduced $CD34^+CD43^+$ pre-HPCs/HPCs from day 8 EBs (Figure 1D). To confirm these findings, we overexpressed *Sox17* in hESC-derived ECs and pre-HPCs/HPCs. Overexpression of *Sox17* also promoted cell growth of hESCs (data not shown). Based on these results, we decided to conduct a detailed analysis of the function of SOX17 using hESCs.

Sox17 promotes expansion of HE-like cells

SOX17 mRNA was highly expressed in EBs between days 2 and 4 of culture (Figure 1E). *SOX17* has been described as one of the master regulator genes for endodermal development.[10,22] High expression of *SOX17* in EBs at early time points supposedly reflects the development of endodermal cells. In contrast, ECs emerged at approximately day 6 in our culture system at the same time as increased expression of hematopoietic regulator genes such as *RUNX1* and *SCL/TAL1* (Figure 1C). Therefore, the expression of *SOX17* after day 6 may indicate a role of *SOX17* in hematopoietic development (Figure 1E). Indeed, *SOX17* was expressed at high levels in ECs, but at significantly lower levels in pre-HPCs, HPCs, and human CB $CD34^+$ cells (Figure 1F). Other *SOXF* family genes, *SOX7* and *SOX18*, showed a very similar pattern of expression profiles (Figure 1F).

To evaluate the effect of overexpression of *Sox17* in hematopoietic development in detail, we produced a retrovirus containing *Sox17* fused to *ERT* (*Sox17-ERT*). We transduced ECs from day 6 EBs with the *Sox17-ERT* retrovirus on OP9 stromal cells and cultured them in the presence of SCF and TPO. The addition of

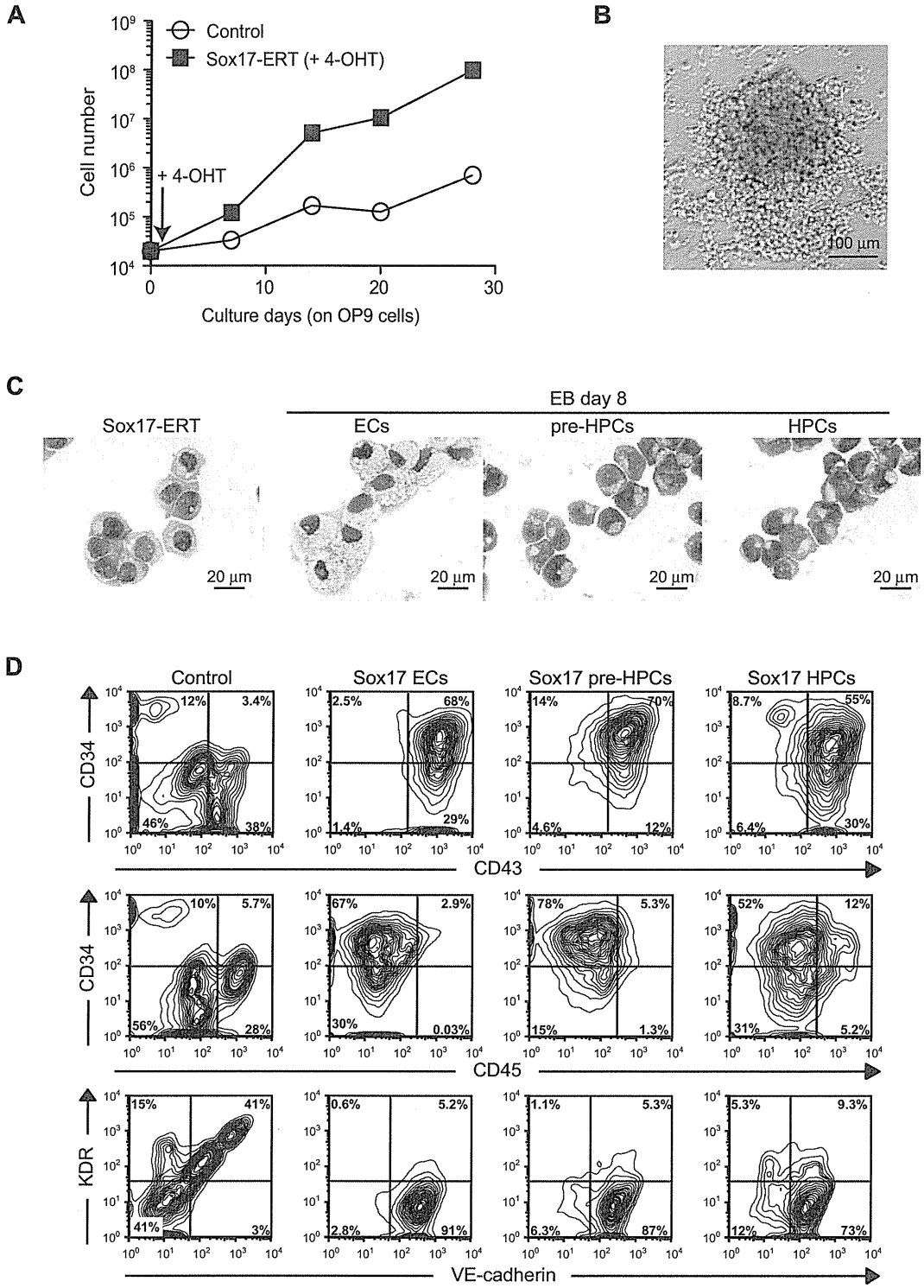

Figure 2. Sox17 promotes the expansion of CD34$^+$CD43$^+$CD45$^{-/low}$ cells. (A) Growth curve of ECs from day 6 EBs that were transduced with a *Sox17-ERT* or a control retrovirus. ECs (2×10^4) were transduced with the indicated retrovirus on OP9 cells and cultured in the presence of 20 ng/mL of SCF and TPO and 200nM 4-OHT. The absolute numbers of cells were determined and plotted. Representative data from repeated experiments are shown. (B) Appearance of a representative colony generated by *Sox17*-overexpressing cells in panel A observed under an inverted microscope. Images were collected using BIOREVO BZ-9000 (KEYENCE) with CFI Plan Fluor ELWD DM 20×C (Nikon). (C) Typical cell morphology of *Sox17*-overexpressing cells in panel A. Sorted cells were cytospun onto glass slides and observed after Wright-Giemsa staining. ECs, pre-HPCs, and HPCs from day 8 EBs served as controls. Images were collected using BIOREVO BZ-9000 (KEYENCE) with CFI Plan ApoVC 100×H (Nikon). (D) Flow cytometric analysis of expanded cells on overexpression of *Sox17*. ECs from day 6 EBs and pre-HPCs and HPCs from day 8 EBs were transduced with a *Sox17-ERT* or a control retrovirus cultured on OP9 in the presence of 20 ng/mL of SCF and TPO and 200nM 4-OHT for 10-15 days and then analyzed for their immunophenotypes.

4-OHT, which induces nuclear translocation of ERT fusion protein, considerably stimulated cell growth (Figure 2A). Overexpression of *Sox17-ERT* promoted cell growth moderately even without 4-OHT, suggesting leaky translocation of Sox17-ERT (data not shown). Indeed, Sox17-ERT was detected in both the nucleus and cytoplasm without 4-OHT, whereas the addition of 4-OHT induced

efficient nuclear translocation of Sox17-ERT (supplemental Figure 1A). *Sox17*-overexpressing cells formed semiadherent cell aggregates on OP9 cells (Figure 2B). Morphologic analysis revealed that they showed a monotonous morphology intermediate between ECs and pre-HPCs (Figure 2C). We performed further immunostaining with an anti-laminin Ab. After incubation in slide chambers for 4 hours, ECs attached to the slide glasses and stretched their cytoplasm out. In contrast, *Sox17*-overexpressing cells behaved like pre-HPCs and maintained a round shape, suggesting that *Sox17*-overexpressing cells do not retain strong adhesive properties of ECs, although they form semiadherent cell aggregates on OP9 cells (supplemental Figure 1B). Flow cytometric analysis demonstrated that *Sox17*-overexpressing cells expanded on OP9 cells were mostly $CD34^+CD43^+$ and did not express or expressed a low level of CD45 ($CD45^{-/low}$). These cells coexpressed the HE producer VE-cadherin (Figure 2D). Interestingly, overexpression of *Sox17* in pre-HPCs and HPCs from day 8 EBs similarly expanded $CD34^+CD43^+CD45^{-/low}$VE-cadherin$^+$ cells (Figure 2D). Although the endothelial-specific marker KDR/FLK1 was expressed in the majority of ECs from day 6 and 8 EBs (data not shown), its expression was immediately down-regulated during differentiation into pre-HPCs and HPCs and also on activation of Sox17 (Figure 2D).

Comprehensive gene-expression analyses using microarrays were performed to investigate the developmental stage of the cells expanded on overexpression of *Sox17*. ECs from day 6 and 8 EBs, pre-HPCs from day 8 EBs, and HPCs from day 8 and 12 EBs were transduced with *Sox17-ERT* and cultured on OP9 cells. These cells were then treated with 4-OHT and the resulting $CD34^+CD43^+CD45^{-/low}$ cells were subjected to microarray analysis. Freshly isolated ECs from day 6, 8, and 12 EBs, pre-HSCs from day 8 EBs, and HPCs from day 8 and 12 EBs served as control samples. The $CD34^+CD43^+CD45^{-/low}$ cells overexpressing *Sox17* appeared to express both EC-related genes such as *VE-cadherin/CDH5* and *ESAM* and hematopoietic-related genes such as *RUNX1* and *SCL/TAL1* (supplemental Table 1). Hierarchical clustering of the cell populations based on the microarray data of total genes revealed that *Sox17*-overexpressing cells showed very similar profiles of gene expression irrespective of the cell sources (ie, ECs, pre-HPCs, and HPCs; Figure 3A). We next performed clustering using probes corresponding to genes identified as "Transcription factor" and "Hemopoiesis" from the GO database. *Sox17*-overexpressing cells were developmentally placed between ECs and pre-HPCs/HPCs (Figure 3B-C). These findings, together with the intermediate morphology between ECs and pre-HPCs, suggest that $CD34^+CD43^+CD45^{-/low}$ cells expanded on the overexpression of *Sox17* are at a developmental stage between HE and early HPCs. To confirm this possibility, we then investigated whether the $CD34^+CD43^+CD45^{-/low}$ cells overexpressing *Sox17* give rise to mature hematopoietic cells on inactivation of Sox17 (Figure 4A). As expected, after depletion of 4-OHT, $CD34^+CD43^+CD45^{-/low}$ cells lost expression of CD34 and VE-cadherin but gained a higher level of CD45 expression and gave rise to $CD235a^+$ erythroblasts and $CD11b^+$ myeloid cells more efficiently than they did in the presence of 4-OHT (Figure 4B-C). This trend was confirmed in colony-forming assays. We seeded $CD34^+CD43^+CD45^{-/low}$ cells overexpressing *Sox17* in methylcellulose medium in the presence and absence of 4-OHT. *Sox17*-overexpressing cells in the presence of 4-OHT mainly formed compact colonies consisting of nonhemoglobinated cells with a morphology similar to ECs (Figure 2B), whereas they generated hemoglobinated erythroid colonies and myeloid colonies in the absence of 4-OHT (Figure 4D). These findings clearly indicate that the $CD34^+CD43^+CD45^{-/low}$ cells overexpressing *Sox17* still retain hemogenic potential, which becomes apparent on removal of 4-OHT.

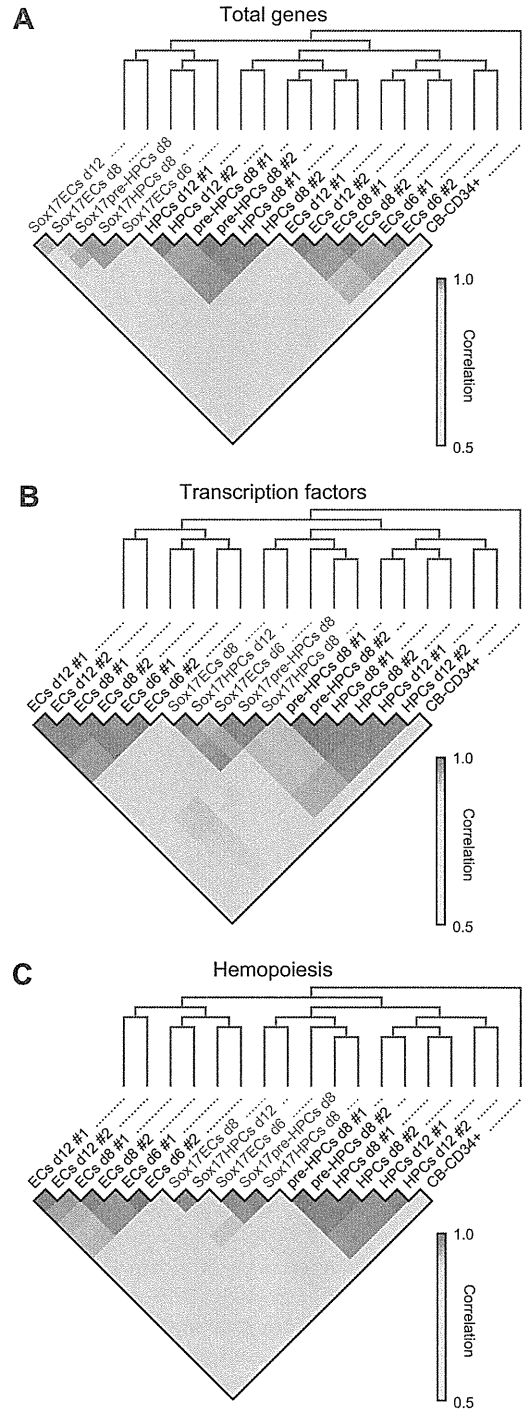

Figure 3. $CD34^+CD43^+CD45^{-/low}$ cells expanded on overexpression of *Sox17* developmentally place between ECs and pre-HPCs/HPCs. Gene-expression patterns of wild-type and *Sox17*-overexpressing cells obtained in microarray analyses were clustered using hierarchical clustering. The distance between 2 samples was defined with the Pearson correlation using total genes (A) or certain probes selected from the GO database (B-C). "Transcription factor" represents genes that are located in the nucleus and have at least 1 of the GO terms "regulation of transcription, DNA-dependent," "transcription factor activity," or "transcription factor complex" (B). "Hemopoiesis" represents genes that are annotated with the GO terms "hemopoiesis," "vasculogenesis," "erythrocyte differentiation," "erythrocyte maturation," and/or "erythrocyte development" (C). The color of each cell represents the value of correlation indicated on the right side of the matrix.

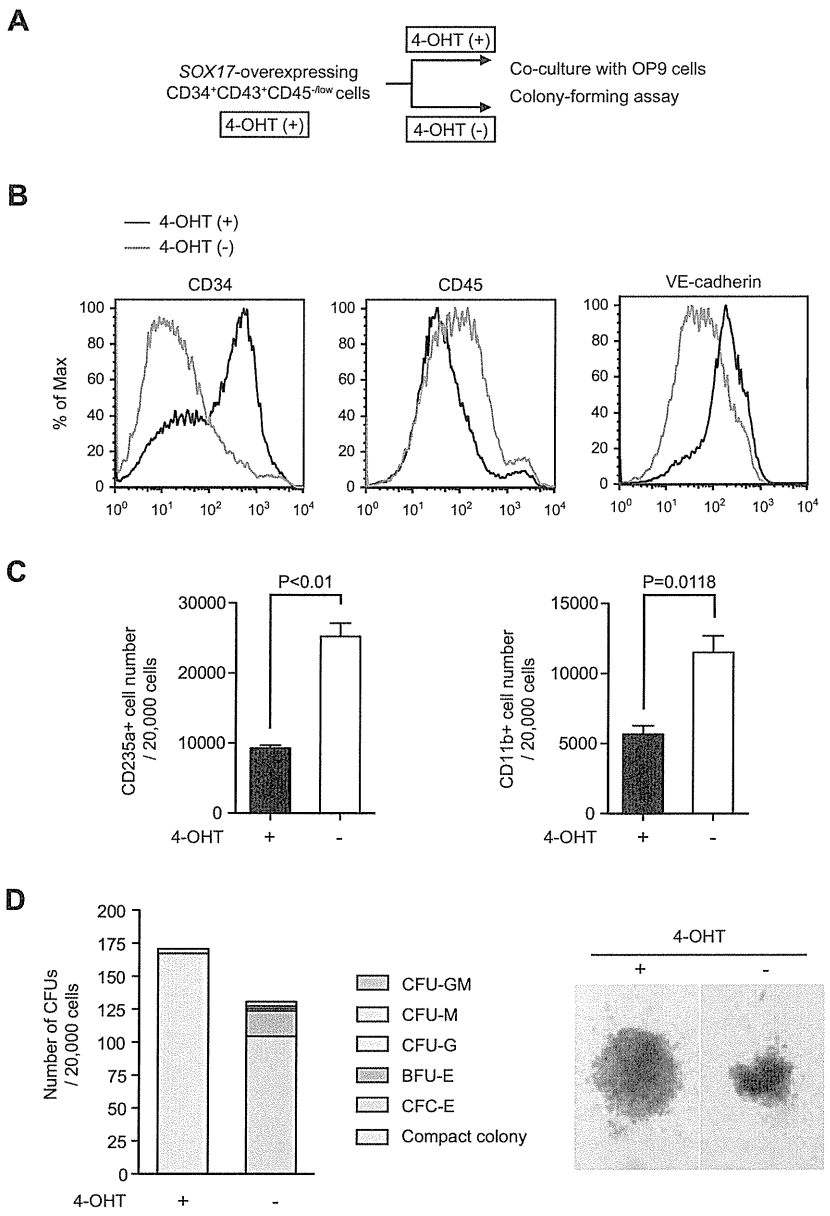

Figure 4. CD34$^+$CD43$^+$CD45$^{-/low}$ cells expanded on overexpression of *Sox17* retain hemogenic potential. (A) Experimental design to evaluate effects of withdrawal of 4-OHT on *Sox17*-overexpressing cells. ECs from day 6 EBs transduced with a *Sox17-ERT* retrovirus were cultured in the presence of 20 ng/mL of SCF and TPO and 200nM 4-OHT for 15 days. Then, the cells were subjected to coculture with OP9 cells and colony-forming assays. For coculture with OP9 cells, the cells were replated onto OP9 cells and cultured in the presence of 20 ng/mL of SCF and TPO, 10 ng/mL of IL-3, and 3 units/mL of erythropoietin with and without 4-oht. at day 7 of culture, the cells were analyzed for their immunophenotypes by Flow cytometry. For colony-forming assays, the cells were replated in methylcellulose in the presence of 20 ng/mL of SCF, 10 ng/mL of TPO and IL-3, and 3 units/mL erythropoietin with and without 4-OHT. At day 12 of culture, the colonies were counted. (B) Representative flow cytometric profiles of cells overexpressing *Sox17-ERT* before and after depletion of 4-OHT. (C) The absolute numbers of CD235$^+$ erythroblasts and CD11b$^+$ myeloid cells in culture at 7 days after depletion of 4-OHT. Data are shown as the means ± SD for triplicate cultures. (D) Ability of *Sox17-ERT*–overexpressing cells to form hematopoietic colonies in methylcellulose cultures with or without 4-OHT. The numbers of CFUs in culture are presented (left panel). CFU-GM, CFU-M, CFU-G, BFU-E, and CFU-E indicate CFU-granulocyte-macrophage, CFU-macrophage, CFU-granulocyte, burst-forming unit-erythroid, and colony-forming unit-erythroid, respectively. Compact colonies indicate colonies composed by HE cell–like cells. The appearance of a representative compact colony and an erythroid colony observed under an inverted microscope is depicted (right panel).

We next compared the expression of globin genes in *Sox17*-overexpressing CD34$^+$CD43$^+$CD45$^{-/low}$ HE-like cells and their hematopoietic progeny with globin gene expression in CB CD34$^+$ cells. CD34$^+$CD43$^+$CD45$^{-/low}$ cells expanded on overexpression of *Sox17* were further cultured in the presence and absence of 4-OHT for 7 days and then GFP$^+$ cells expressing *Sox17-ERT* were collected by cell sorting. RT-PCR analysis revealed that embryonic globin (ε) and fetal globin (γ), but not adult globin (β), were highly expressed in *Sox17*-overexpressing cells and/or their hematopoietic progeny (supplemental Figure 2). These results raise the possibility that the CD34$^+$CD43$^+$CD45$^{-/low}$ HE-like cells expanded on overexpression of *Sox17* are a hemogenic intermediate differentiated from hemangioblasts that primarily give rise to yolk sac–type blood cells.[8]

SOX17 is essential for the hemogenic activity of HE cells

Our results so far indicate that the overexpression of *Sox17* promotes the expansion of HE-like cells, but inhibits their hematopoietic differentiation into pre-HPCs. Because *SOX17* is highly expressed in ECs enriched in HE, we examined the role of SOX17 by knock-down analysis. We transduced ECs from day 5 EBs with lentiviruses expressing shRNA against *SOX17* on OP9 cells and allowed them to differentiate into hematopoietic cells for 9 days. The most effective shRNA, sh-*SOX17*#1273 (Figure 5A), suppressed the development and differentiation of hematopoietic cells including both erythroblasts and myeloid cells significantly, whereas it only moderately diminished the growth of CD235a$^-$CD11b$^-$ nonhematopoietic cells, the majority of which do not express SOX17 even though approximately 25%-30% of these cells are SOX17$^+$ ECs (Figure 5B-C). sh-*SOX17*#1143 similarly, albeit modestly, suppressed the production of hematopoietic cells. Similar results were obtained when we knocked down *SOX17* in ECs from day 6 EBs (data not shown). However, hematopoietic differentiation was not affected on *SOX17* knock-down in pre-HPCs from day 8 EBs (Figure 5D). These findings indicate that SOX17 plays a key role in the acquisition of hematopoietic potential in HE cells.